Final Report

1. DOE Award: DE-SC0001055

   Institution: GE Global Research
   One Research Circle, Niskayuna, NY 12309

   Partners: Lawrence Berkeley National laboratory

   Stanford University

   Yale University

2. Project Title: Center for Electrocatalysis, Transport Phenomena, and Materials (CETM) for Innovative Energy Storage

   Director: Dr. Grigorii Soloveichik

   Date of Report: November 30, 2014

   Period covered by report: August 1, 2009 – October 30, 2014

   DOE Program Manager:
   Dr. Craig Henderson
   SC-22.2/Germantown Building
   U.S. Department of Energy
   1000 Independence Avenue, SW
   Washington, D.C. 20585-1290

3. Executive Summary

EFRC vision. The direct use of organic hydrides in fuel cells as virtual hydrogen carriers that generate stable organic molecules, protons, and electrons upon electro-oxidation and can be electrochemically charged by re-hydrogenating the oxidized carrier was the major focus of the Center for Electrocatalysis, Transport Phenomena and Materials for Innovative Energy Storage (EFRC-ETM). Compared to a hydrogen-on-demand design that includes thermal decomposition of organic hydrides in a catalytic reactor, the proposed approach is much simpler and does not require additional dehydrogenation catalysts or heat exchangers. Further, this approach utilizes the advantages of a flow battery (i.e., separation of power and energy, ease of transport and storage of liquid fuels) with fuels that have system energy densities similar to current hydrogen PEM fuel cells.

EFRC challenges. Two major EFRC challenges were electrocatalysis and transport phenomena. The electrocatalysis challenge addresses fundamental processes which occur at a single molecular catalyst (microscopic level) and involve electron and proton transfer between the hydrogen rich and hydrogen depleted forms of organic liquid fuel and the catalyst. To form stable, non-radical dehydrogenation products from the organic liquid fuel, it is necessary to ensure fast transport of at least two electrons and two protons (per double bond formation). The same is true for the reverse hydrogenation reaction. The transport phenomena challenge addresses transport of electrons to/from the electrocatalyst and the current collector as well as protons across the polymer membrane. Additionally it addresses prevention of organic liquid fuel, water and oxygen transport through the PEM. In this challenge, the transport of protons or molecules involves multiple sites or a continuum (macroscopic level) and water serves as a proton conducting medium for the majority of known sulfonic acid based PEMs. Proton transfer in the presence of prospective organic liquid fuels was studied.

During EFRC program various types of electrocatalysts, classes of fuels, and membranes have been investigated.

Fuel selection. For different fuel classes (e.g., carbocyclic fuels, O- and N- heterocyclic fuels and oxygenates) we developed and verified an accurate computational tool for the calculation of thermodynamic properties and fuel redox potentials. This tool enabled the identification of potential fuels with high energy densities (1100 - 1650 Wh/L), some of which have theoretical open circuit potentials higher than that of the hydrogen fuel cell. Fuel cells using organic fuels have the theoretical maximum efficiency in the range of 93 – 95% at 80°C (83% for hydrogen fuel cells) and may be competitive for mobile energy storage as well as stationary applications owing to their high potential and theoretical efficiencies.

The structure property relationship of the organic liquid fuel and the oxidation potential, as well as the nature of the products formed by electrooxidation in the absence of a catalyst at a bare electrode was esttablished. Tuning the oxidation potential of organic liquid fuels via the addition of substituents was demonstrated. Bases were employed to enhance the rate of the electrooxidation and lower the oxidation onset potential for liquid organic fuels and the mechanism of the base effect was elucidated.

Transport phenomena study and membrane selection. Study of the mechanism of proton and fuel transport in PEMs in the presence of fuels resulted in design criteria for selection of compatible fuel-membrane couples. Using the dynamic relaxation, mechanical and morphological properties of commercially available acidic membranes plasticized with candidate fuels allowed for the understanding of the effect of fuel-electrolyte-polymer interactions. Hydrocarbon cyclic fuels interact with the hydrophobic polymer backbone changing the membrane morphology in such a way that preserves high proton conductivity at low relative humidities and reduces the hydrogen crossover. This effect led to substantial power density increase for hydrogen-oxygen fuel cells.

Computational tools development. Theoretical models for redox potentials, both of fuel molecules and electrocatalysts were developed. These models were used for calculation of redox potentials of transition metal complexes and demonstrated the ability to predictably adjust those redox potentials using structure activity relationships within at least 600 mV range. These tools were also used to evaluate pathways for different catalytic cycles and illustrated the benefit of using non-innocent ligands for two proton/two electron transfer in the electrocatalytic dehydrogenation of chemical fuels.

Electrocatalysis. The use of outer sphere electrocatalysts (ferrocenes, NNN cobalt complexes) resulted in formation of mostly radical products of one-electron oxidation. Addition of a strong base only slightly improved reaction selectivity towards dehydrogenation.

Quinones with high oxidation potential can be used as electrocatalysts in oxidation of N-containing fuels via formation of pi-complexes with substrates. While this strategy successfully demonstrates the effectiveness of using an inner sphere electrocatalyst (selective product formation) the relatively high redox potential and slow reaction kinetics of quinones suggests that they are not practical electrocatalysts in the context of an organic fuel cell.

Our initial hypothesis of using thermal dehydrogenation catalysts as electrocatalysts turned out to be only partially true. In many cases these catalysts were inactive in electrooxidation. Computational study of electrooxidation mechanisms indicated that the formation of intermediate species with negative redox potentials broke the catalytic cycle.

Theoretical and electrochemical analyses of electrocatalysis by rhodium(II) cationic complexes established an inverse dependence of the acidity and hydricity of an intermediate hydride on the nature of the chelating ligand. This theoretical model predicted a ligand environment which, when implemented, enhanced the overall electrocatalytic efficiency of the rhodium(III) catalyst system.

Iridium catalysts with non-innocent ligands that showed excellent selectivity and Faradaic yields in the oxidation of alcohols were developed. The iridium system demonstrated the desired separation of protons and electrons with a homogeneous catalyst system used in the electrochemical dehydrogenation of fuels.

Understanding parameters controlling activity in both directions (reversibility) is extremely important for development of rechargeable fuel cells. With the current iridium system, the concept of utilizing microscopic reversibility was extended to electrocatalysis by employing the same electrocatalyst precursor with a base/conjugate acid pair in the presence of the appropriate metallocenes as oxidizing and reducing agents for the electrochemical dehydrogenation/hydrogenation of a fuel/spent fuel combination has been demonstrated.

Electro-dehydrogenation and -hydrogenation reactions with first row transition metal electrocatalysts, nickel pincer complexes, were discovered. The microscopic reversibility principle was also demonstrated in reversible acceptorless dehydrogenation of alcohols effectively catalyzed by an iron complex with non-innocent ligand.

Method for immobilization of molecular complexes of transition metals on practical conductive carbon surfaces via attaching reactive azide groups followed by tethering catalysts through “click” chemistry has been greatly improved. As a result, very high surface concentrations of tethered metal complexes were that exhibited high rates of electron transfer and unchanged electrochemical properties were achieved.

Further work based on the EFRC-ETM results can be eventually translated into design criteria for the envisioned innovative energy storage and delivery system

4. Comparison of Actual Accomplishments with the EFRC Goals and Objectives

To compare the actual EFRC accomplishments with the goals and objectives, this section is organized by challenge areas refined for this EFRC during the course of the project. To reach the EFRC ultimate goal – develop a fundamental basis for a regenerative organic fuel cell/flow battery combination for energy storage – it is necessary to understand the mechanism of electron and proton transfer between a fuel and a catalytic center at the microscopic level (electrocatalysis challenge), the mechanism of proton transfer and membrane/fuel interaction at the macroscopic level (transport phenomena challenge), and the interaction of all components in a fuel cell at the micro/macro level junctions (integration challenge). Below our accomplishments are compared with the EFRC goals and objectives. For the past 9 months part of the work was funded by a complementary grant from NYSTAR-EDS to support EFRC work, and main results are reflected in this report.

Electrocatalysis Challenge (GE, Yale, LBNL, Stanford, UC Berkeley, University of Rochester)

For the **electrocatalysis challenge,** we planned to identify organic carriers with high energy storage capacity and develop viable synthetic methods, and to demonstrate the simultaneous, selective two-electron, two-proton transfer in electrocatalytic dehydrogenation of organic carrierss and the electrochemical reversibility of this reaction. We identified a knowledge gap in the understanding of the thermodynamics and electrochemical properties of plausible organic liquid fuels. The goal was to compute absolute values of redox potentials in the condensed phase with a focus on carbocyclic and oxygenated fuels compatible with practical proton exchange membranes. We planned to study the combination of substituent and base effects on the electro-oxidation of nitrogen heterocycles. We aimed to elucidate the mechanism for the electrochemical dehydrogenation of alcohols starting with iridium complexes containing non-innocent ligands. For enhanced activity and reversibility, we aimed to facilitate proton removal by incorporating basic sites into the framework of redox-active ligands. We also planned to explore non-platinum group metals as electrocatalysts in dehydrogenation/hydrogenation of various fuels. In addition, we intended to evaluate the applicability towards practical, energy dense fuels for the rechargeable fuel cell/flow battery.

The **organic carrier study** allowed for identification of suitable classes of organic carriers and for selection of promising fuels with high energy density.

<u>Selection of organic carriers based on computational approach</u>

- DFT molecular modeling was performed to develop structure - property relationships for the dehydrogenation of organic carriers. Gibbs free energy of the dehydrogenation reaction was calculated from total energies of the starting heterocyclic molecules and the resulting dehydrogenated molecules in vacuum.
- The modeling work and comparison to thermodynamic values obtained from the literature and NIST database showed a correlation between calculated and experimental values. Open circuit potential of organic fuel cells was accurately predicted.
- It was found that the products derived from aromatization of the dehydrogenated products were more favorable than products that contain only conjugation of double bonds. The 1,3 arrangement of nitrogen atoms in a heterocycle had the tendency to lower the free energy of hydrogenation.

<u>Synthesis of organic carriers</u>

- Synthetic methods for selected saturated and unsaturated.heterocycles (2-alkylquinoxaline, N-alkyl-1,8-pyrrolopyridine, 9-alkyloctahydropurine, imidazoles and azacarbazoles) were developed (no published synthetic routes found). The subsequent hydrogenation of heteroaromatics to saturated heterocycles requires selection of the catalyst and reaction condition to avoid excessive hydrogenolysis of the C-N bond.

- Our model fuel, dodecahydro-N-ethylcarbazole (not commercially available, but an excellent candidate fuel based on calculations described above) has been prepared by high-pressure hydrogenation of N-ethylcarbazole in a one hundred-gram scale. This fuel was employed at all EFRC facilities for testing catalysts and membranes.
- Promising organic carriers that could yield theoretical OCPs higher than that for the hydrogen fuel cell were identified including high energy density C-B-N heterocycles
- Non-flammable oxygenated fuels with energy density 1100 – 1650 Wh/L were selected for electrocatalysts and fuel cell development.

Electrooxidation of model fuels

- In electrooxidation of N-heterocycles , the base (added to aid in proton abstraction from oxidation intermediates) played a critical role in the observed behavior. The fuel structure (i.e. position of the N hetero atom in the ring), the relative basicity of fuel and base as well as additional functional groups on the fuel to prevent or direct potential side reactions were identified as key parameters. The mechanism of a base effect on the redox potential of fuels via formation of hydrogen bonds was elucidated and quantified.
- An accurate computational tool for the calculation of fuel redox potentials was developed and verified.
- We found that the electrochemical mechanism changes with the fuel and base concentration from CECE leading to formation of oligomers via radical intermediates to CEEC resulting in increased formation of dehydrogenation products.
- The use of ferrocene as an outer sphere electrocatalyst in electrooxidation of indoline and *N*-ethyldodecahydrocarbazole resulted in modest increase of current indicating a weak catalysis. In the presence of strong bases (e.g. imidazole) the selectivity towards dehydrogenated products reached 50%.
- A potential fuel candidate, N-ethyldodeca-hydrocarbazole (NEC-H12), and the major possible intermediates in its dehydrogenation to N-ethylcarbazole, octahydro- (NEC-H8) and tetrahydro- (NEC-H4) have been prepared at the tens of grams scale and studied by cyclic voltammetry. Ferrocenes catalyze NEC-H12 and NEC-H8 electrooxidation to NEC in the presence of a strong base, but are inactive towards NEC-H4 oxidation, which exhibits more positive oxidation potential. These data correlate with DFT calculation of the first oxidation potentials of saturated and aromatic N-heterocycles.
- A high-temperature (up to 145^{o}C) cyclic voltammetry method using coordinating and non-coordinating solvents was developed.

In the **electrocatalysis area** we demonstrated the separation of protons and electrons using homogeneous catalysts that led to the electrocatalytical dehydrogenation of fuels. Several classes of outer sphere catalyst and inner sphere electrocatlysts including organic redox active compounds, pincer complexes of the first row transition metals and complexes with non-innocent ligands were found to exhibit electrocatalytic properties. For iridium based catalyst, microscopic reversibility was confirmed using several couples of base/conjugate acid with the appropriate reducing and oxidizing agents. Microscopic reversibility in the chemical dehydrogenation reaction was also demonstrated for first row transition metal (Fe) catalysts. To assist in further catalyst development, we have improved methods for quantitative prediction of pKa and redox potentials of fuels and electrocatalysts, helpful in identifying the most probable reaction pathways.

Prediction and tuning redox potentials of metal complexes

- Computational method for accurate computation of redox potentials of transition metal complexes with a mean of -2 mV and a standard deviation of 64 mV at moderate cost was developed
- Placing electron donating or withdrawing substituents in ligands allows for tuning the redox potential of metal complexes in the range of more than 600 mV.

Dehydrogenation of azaheterocycles using organic electrocatalysts

- New concept of organocatalysis for the dehydrogenation of saturated azaheterocycles has been developed. This avoids the problems of hydrogen evolution that would plausibly be encountered with metal catalysts as well as high catalyst costs. Quinones are preferred for oxidation and dihydropyridines for reduction; in each case electrochemical regeneration of the oxidant or reductant is in principle possible

Outer sphere electrocatalysts in dehydrogenation of organic carriers

- Electrochemistry of a series of chelate complexes of iron, cobalt and nickel has been studied in solution and with addition of decalin as a model organic carrier, decalin. It was found that some cobalt complexes catalyze oxidation of decalin at potentials substantially lower than that for non-catalytic decalin oxidation as seen by a sharp increase of the catalytic current. Iron and nickel complexes with the same ligands are catalytically inactive. This is the first example of electrocatalytic oxidation of a hydrocarbon by a cobalt complex. Mechanism and oxidation products of decalin and other carriers showed outer sphere oxidation with formation of products of radical transformations.

Synthesis and eletrocatalytic activity of transition metal pincer complexes

- Based on a thorough literature analysis, transition metal complexes capable to activate the C-H bond have been selected as starting point for development of electrocatalysts. Pincer complexes of PCP, PNP, NCP, NNN and other chelate ligands with iridium, rhodium, nickel have been synthesized and characterized.
- DFT B3LYP electronic structure calculation methods were applied to analyze the underlying reaction pathways in terms of the characterization of catalytic reaction intermediates for Ir PCP pincer complexes. Standard redox potentials of metal hydrides and solvo complexes have been calculated. The comparative analysis of structural stability for various reaction intermediates indicates that the Ir PCP pincer complex 18-electron tetrahydride form is the most stable form of the while the 16-electron dihydride intermediate is the catalytically active state.
- Computational studies of Ni(II) terpyridyl complexes show catalytic activity (i.e., a reduction of potential energy barriers) for the catalytic hydrogenation of model alkenes as compared to the uncatalyzed hydrogenation (i.e., activation barrier is reduced from ΔG(aq) = 92.7 to 32.3 kcal mol-1 for ethylene hydrogenation. Formation of a hydride intermediate and the presence of a base further reduce the activation barriers.
- Identified nickel NNN pincer catalysts that can hydrogenate organic fuels and produce hydrogen at low overpotential which is assisted by proton transfer to the ligand. The acidity of reduced Ni electrocatalysts with redox-active ligands was measured using pulse radiolysis in collaboration with BNL.
- Incorporation of a quinoid group into a NHC carbene ligand allowed the electrocatalytic activity of Ni complexes to exceed the activity of similar complexes with an external quinone.
- Nickel-based chloride and hydride complexes with tunable electronic and steric properties were synthesized employing chelating ligands. Electron-donating or –withdrawing substituents at the para position of the aromatic ring of the ligand allowed tuning of the oxidation potential.

(POCOP)NiCl and (POCOP)NiH complexes are electrochemically well-behaved and they show reversible $Ni^{II/III}$ redox processes in acetonitrile.

Electrocatalytic properties of iridium complexes with non-innocent ligands.

- Demonstrated separation of proton and electron transfer processes in the catalytic dehydrogenation of primary alcohols using Grützmacher's $[Ir(trop_2DACH)]^+$ and $[Ir(trop_2DAD)]^+$ complexes.
- Mechanism of the $[Ir(trop_2DACH)]^+$ catalyst activation via ligand deprotonation is being elucidated.
- Selective electrocatalytic dehydrogenation of primary alcohols to aldehydes via transfer of two electrons and two protons demonstrated.
- Selection of a non-coordinating solvent (1,2-difluorobenzene) and optimization of a base and electrolysis condition allowed for >98% faradaic efficiency in electrooxidation of 4-methoxybenzyl alcohol.
- Demonstrated microscopic dehydrogenation/hydrogenation reversibility between 1-octanol and octyl aldehyde using $[Ir(trop_2DAD)]^+$ as a catalyst. The forward and reverse reactions are carried out with the same catalyst and the same base (phenolate)/conjugate acid (phenol) using metallocenes as the oxidizing (ferrocenium) and reducing (cobaltocene) agents.

Understanding of electrochemical properties of metal hydrides.

- Demonstrated two electron redox activity and tunability of redox potentials due to modular synthesis through the electrochemical study of potential electrocatalysts $[Cp^*Rh(chelate)(MeCN)]^{2+}$; isolated and characterized the reduced electrocatalysts, Cp*Rh(bpy) and Cp*Rh(phen).
- Computational analysis and cyclic voltammetry of the $(PCP)Rh^{I}(H_2)$ (PCP = κ3-C_6H_3-2,6-$(CH_2P(^tBu_2))$ complex in acetonitrile (MeCN), dimethylsulfoxide (DMSO) and 1,2-difluorobenzene (1,2-DFB) elucidated the mechanism of electrooxidation. In weakly or non-coordinating media such as 0.05 M $NaBAr^F_4$ in 1,2-DFB it is a simple one electron oxidation to $[(PCP)Rh^{II}(H_2)]^+$. Conversely, in coordinating solvents (e.g. MeCN and DMSO) the reactivity is dominated by solvent coordinated species with a slight variation in the $Rh^{III/II}$ oxidation potentials as a function of the supporting electrolyte conductivity.
- Demonstrated electrocatalyic activity of $[Cp^*Rh(bpy)(MeCN)]^{2+}$ in the dehydrogenation of formate.
- It was found that electrochemical and chemical oxidation of (POCOP)NiH complexes leads to H_2 evolution via a bimolecular acid-base mechanism (ECE or E-CPET).
- Understanding the proposed inner sphere mechanism for electrocatalytic dehydrogenation allowed to develop means for control of dehydrogenation pathways vs. radical pathways for Cp*Rh complexes. It was consistent with modeled fuel ligation to the metal center and synthesis of a stable metal-fuel adduct for the first row analogue. The formation of an elusive rhodium hydride was observed via ^1H NMR spectroscopy and confirmed the mechanism.
- DFT calculations of the transfer hydrogenation catalyzed by Baratta's $(NNC)RuL_2H$ catalyst correlate with experimental data and are consistent with a mechanism involving ketone insertion into the Ru-H bond. The effects of cis- and trans-ligands on the catalytic activity were accurately predicted using this model.

Computational study of electrocatalysts.

- Developed DFT method for calculation of the redox potential of transition metal complexes using an appropriate internal reference couple provides accurate computation of the redox potentials with a standard deviation of 64 mV at moderate computational cost
- An inverse design algorithm offers efficient search for ligand modification of a reference catalyst framework via minimization of differences between reaction energies or barriers through continuous structure variation
- DFT and temperature-dependent paramagnetic ^{1}H NMR of a tridentate NNN Ni^{II} complex, an electrocatalyst for aqueous H_2 production at low overpotentials, and its diamagnetic Zn analogue complex shown that the NMR T_1 relaxation rates, temperature dependence of the chemical shifts, and dc SQUID magnetic susceptibility correlate to DFT chemical shifts and provide an unambiguous assignment of the six proton environments in the NNN ligand.
- The demonstrated NMR/DFT methodology could be used in the search for appropriate ligands of 3d metal complexes with optimized reactivity.

Immobilization of electrocatalysts on a conductive surface

- Click chemistry method for tethering of metal complexes to various carbon surfaces including carbon powder (Vulcan XC-72R) developed. Species with appended ethynyl groups (-C≡CH) can be covalently attached to the carbon surfaces under ambient conditions in aqueous or organic solvents catalyzed by a variety of Cu(I) complexes.
- The kinetics of the Cu(I)-catalyzed azide alkyne cycloaddition reaction have been investigated on both azide-terminated carbon surfaces and on azide-terminated alkane thiol monolayers on gold to understand the requirements for rapid and selective immobilization of electrocatalysts.
- Catalytic activity of tethered Fc found to be comparable with homogeneous activity
- Electron transfer rates for ferrocene with different chemical linkers measured

Transport Phenomena and Integration Challenge (GE, LBNL, Stanford, Yale)

In the **transport phenomena challenge** we aimed studying the compatibility of fuels with membrane systems that have different backbones and acidity. A shift towards alcohols as substrates was based on electrocatalytic systems that have shown promising results. We also planned to continue modifications to membranes that provide chemical selectivity towards the nitrogen heterocycles, as it is observed that the conductivity of the membranes in the presence of excess base remains practical. We intended to probe the fuel induced changes in membrane morphology using SAXS and solid state NMR and correlate the PEM morphology with the proton diffusion in the presence of high concentrations of fuels. We also planned to explore chemical modification of the hydrogen carrier fuels such as sulfonation to convert them to anionic compounds that the cation exchange membranes will reject.

In the **transport phenomena area**, the main accomplishments are the identification of compatible fuel/membrane combinations based on the study of the interaction of fuels with PEMs. We also reduced the fuel crossover via modification of a proton conducting medium and evaluated the plasticizing effect of fuels on proton exchange membranes. Novel monomers for polybenzimidazole based PEm provided better conductivity and oxidative stability.

Selection of membranes for organic fuel cells

- Analysis of the solubility parameters was used for selection of promising proton exchange membranes. Commercial and experimental membrane materials have been evaluated as starting backbones: perfluorosulfonate polymers such as Nafion® and Aquivion® resins, polybenzimidazole resins imbibed with phosphoric acid, and sulfonated polyethers such as perfluorosulfonated polyarylethers and sulfonated polysulfone. The analysis of these membranes suggests that PEMs most resistant to organic fuel crossover should be those with higher solubility parameters than Nafion®.

- Several fuel-electrolyte pairs that are outside of the interaction radius of polybenzimidazole polymeric scaffold have been identified and the solubility space distances for a number of model fuels-electrolytes which should have low crossover have been calculated.
- Imidazole and phosphoric acid were selected as non-aqueous proton carriers along with polybenzimidazole and polysulfone backbones

Development of anhydrous proton exchange membranes containing heterocyclic bases.

- Work on anhydrous membrane materials containing heterocyclic bases has shown that some level of plasticization by water or organic carriers will be necessary to obtain high conductivity. The degree of molecular organization required to provide connectivity through the bulk material is not feasible at present. However, it has been noted that some chemical functionalities can be included in to the membrane structure to enhance selectivity.

Development of anhydrous proton exchange membranes containing phosphoric acid and polybenzimidazole backbone..

- Increasing the mechanical strength and oxidative stability of polybenzimidazoles was done by inclusion of sulfone functionality. We have synthesized the monomer 4,4'-sulfonylbis(1,2-benzenediamine) via an initial fluoro-displacement reaction on 4,4'-difluoro-3,3'-dinitrophenylsulfone with ammonium hydroxide to produce the 4,4'-diamino-3,3'-dinitrophenylsulfone followed by catalytic hydrogenation to produce the desired monomer. We have also synthesized an electron deficient monomer 4-(3,4-diaminophenylsulfonyl)benzoic acid via a 4 step process.

Effect of PFSA membrane modification with proton conductors and fuels.

- Modification of commercial PFSA membranes such as Nafion™, Aquivion™ and a 3M membrane with hydroxymethylimidazole significantly improved selectivity of the membranes while only moderately reducing the conductivity at high relative humidities. Conductivity results for Nafion modified with hydroxymethylimidazole (Fig. 2) clearly demonstrate that the nature of the nitrogen base is critical as well as the concentration. Crucially, these modified membranes exhibit high selectivity for transport of methanol through the membranes.
- Water uptake studies and SAXS measurements on the modified membranes show that the water uptake is lower and the morphology changes limit swelling with water. These results are corroborated by the NMR measurements that indicate slower diffusion of water and methanol.
- The diffusion coefficient of water and methanol, as determined by pulsed field gradient (PFG) NMR with stimulated echoes, is lower in modified membranes than in standard ones. The lower diffusion of the species in a substance correlates with observed greater membrane resistance. The relation between diffusion of a species and its crossover are directly proportional, meaning the modified membranes should experience lower methanol crossover and therefore become more prime candidates for direct fuel cell membrane material.
- A method for substantial reduction of the membrane resistance while preserving high fuel selectivity of modified membranes was developed. When a modified membrane is sandwiched between thin conventional unmodified Nafion® membranes, the contact resistance decreased for 3-4 times.

Membrane backbone modification.

Elucidation of polybenzimidazole microstructure.

- NMR evaluation of the microstructure of *m*-polybenzimidazole (*m*-PBI), the condensation polymer of 3,3'-diaminobenzidine and isophthalic acid, was done using ^{1}H- and ^{13}C-NMR spectroscopy in a variety of deuterated polar aprotic solvents.

- Unexpectedly, aryl-substituted 2-aminoaniline endgroups from incompletely polymerized diaminobenzidine were not observed.
- Number average molecular weights (M_ns), determined from endgroup analysis, qualitatively tracked M_ws calculated from viscometry of dilute *m*-PBI/H_2SO_4 solutions.
- The relative molar ratio of dibenzimidazole tautomers was determined to be 1.0:2.5:1.6 (5,5'-/5,6'-/6,6'-) and matched DFT-calculations of model compounds.
- Activation energy of 17.2 kJ/mol for benzimidazole tautomerization was determined.

Adjusting membrane pH and fuel pKa.

- With NYSTAR funding, Na^+ conducting membranes were prepared by soaking commercial N212 membranes in NaOH at 80^0C. The ionic conductivities were measured at a range of temperatures and were in the range of 9-12 mS/cm at 95% RH.
- Testing of a Na^+ conducting N212membrane in a fuel cell with 1M isopropanol fuel /0.5M NaOH showed an OCV of 0.9V and current density 10 mA/cm^2 at 0.4V at room temperature.
- Anionic derivatives of tetrahydrocarbazole with carboxylic or sulfonic acid side chain attached to the nitrogen atom, which less interact with PFSA membrane, were synthesized via nucleophilic substitution with a good yield.

For the **integration challenge** we planned to evaluate the applicability of catalytic systems heterogenized on a carbon surface for flow cell and fuel cell systems and demonstrate the EFRC concept using liquid fuels. Integration of electrocatalysts, mediators and modified surfaces into operating cells will allow measuring the properties of our catalysts and membranes, e.g. crossover of the high concentration fuels through the bulk membranes, under conditions closer to practical systems. To ensure the catalyst stability, we intended to explore adjusting the pH environment of the PEM via addition of an anion-exchange ionomer to the catalytic layer.

In the **integration area**, we determined the fuel compatibility with proton conducting membranes, developed reproducible methods for the support modification and the catalyst immobilization, and demonstrated the fuel electrocatalytic oxidation in a flow cell.

Fuel – membrane compatibility.

- Compatibility of different classes of promising fuels: cyclic hydrocarbons, nitrogen- and oxygen-containing heterocycles, and alcohols with proton conducting membranes was evaluated and compatible fuel-membrane couples were selected. Though cyclic hydrocarbons are the most compatible, they are the most difficult to activate. Therefore alcohols (diols) were selected fuels for organic fuel cells as having the best combination of membrane compatibility and activity in electrochemical oxidation.

Catalyst support modification.

- An inexpensive method for attaching functional groups to the multi-walled carbon nanotube (MWCNT) surface via hydrothermal polymerization of carbohydrates followed by carbonization was developed. MEAs with MWCNT grafted with allyl group on the surface demonstrated a current density in a hydrogen fuel cell 2.5 times higher compared to conventional XR-72C support.

Catalyst immobilization.

- The reproducible, scalable, and chemically-specific azide functionalization of high surface area carbon Vulcan XC-72R powder with coverage of 1.4 x 10^{14} azides/cm^2, the highest functional group coverage on a porous carbon surface, was achieved by treatment with gaseous IN_3.
- Further carbon surface functionalization with a metal complex, ethynylferrocene, has been accomplished through cycloaddition with terminal alkynes species through formation of a 1,2,3-

triazole linker. An electron-transfer rate through the linker for the immobilized ferrocene was measured electrochemically as greater than 100 s^{-1}.

- A spray coating technique allowed catalysts (decamethyl ferrocene) as well as base modifiers (tetramethylguanidine) to be incorporated in the electrode layers and MEAs to be prepared with these modified membranes.

Catalyst testing in a flow cell.

- Fully integrated catalysts and bases with modified membranes were tested in a fuel cell using indoline as the fuel to produce small current densities. It was found that the indoline binds to the platinum catalysts in the cathode of the cell. The system requires the use of different fuels as well as different catalyst to provide optimum performance.

5. Highlighted Accomplishments and Research Plans

In this section technical results showing the progress made over the course of the project are highlighted in more detail.

SELECTION OF ORGANIC HYDROGEN CARRIERS

Using a combination of theory and experiments we have developed a fundamental understanding of fuel properties to maximize power output of an organic liquid fuel cell.

Molecular modeling (Spartan 2008 and Gaussian 09 software packages, DFT method B3LYP with basis set 6-311++G**) was performed to develop structure - property relationships for the dehydrogenation of organic carriers. Gibbs free energy of the dehydrogenation reaction was calculated from total energies of the starting heterocyclic molecules and the resulting dehydrogenated molecules in vacuum. It was found that the products derived from aromatization of the dehydrogenated products were about 3 kcal/mol H_2 more favorable than products that contain only conjugation of double bonds (Fig. 1). From several dozen studied molecules, the 1,3 arrangement of nitrogen atoms in a heterocycle had the tendency to lower the free energy of hydrogenation. Examples of molecules with low ΔG of dehydrogenation include 1,8-pyrrolopyridine (11.9 kcal/mol) and 9-alkyloctahydropurine (9.8 kcal/mol H_2).

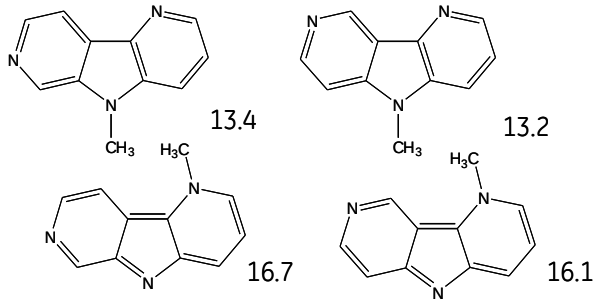

Figure 1. ΔG dehydrogenation (in kcal/mol H_2) of dehydrogenation of N-heterocyclic isomers to aromatic and conjugated compounds.

In order to maximize the organic fuel cell energy density, we need a cell potential that is close to or exceeds the cell potential for the hydrogen fuel cell (1.23 V). To predict theoretical energy densities, we have calculated the thermodynamic open circuit potential (OCP) of fuel cells based on reaction (Eq. 1), where LH_n is hydrogenated and L is dehydrogenated fuel, for several organic fuels from the NIST thermodynamic database. It was found that the thermodynamic OCP for organic fuel cells with cyclic organic carriers are in the range of 0.83 – 1.13 V. When organic carriers are dehydrogenated to non-aromatic, unsaturated products, the OCP is in the range of 0.83 – 0.88V, but increases to 1.08 - 1.13 V when dehydrogenated products are aromatic (Fig. 2a). We have chosen organic carriers that form aromatic dehydrogenation products based on their more favorable OCP. In contrast to the hydrogen fuel cell, increasing the working cell temperature does not necessarily decrease the cell OCP (Fig. 2b). Consequently, elevated temperature operations might be beneficial for organic flow battery/fuel cells.

$$LH_n + n/2\ O_2 \leftrightarrow L + n/2\ H_2O \qquad (1)$$

LH_n: hydrogenated fuel; **L**: dehydrogenated fuel

Experimental thermodynamic parameters for organic carriers in the condensed state, especially for non-aromatic compounds, are scarce. Several gas phase computational methods for calculation of E^0 of cells based on reaction (1) for 22 model carriers have been benchmarked vs. NIST thermodynamic data, and the DFT B3LYP method with 6-311++G** basis set provided good linear trending ($R^2 = 0.99$) (Fig. 2a).

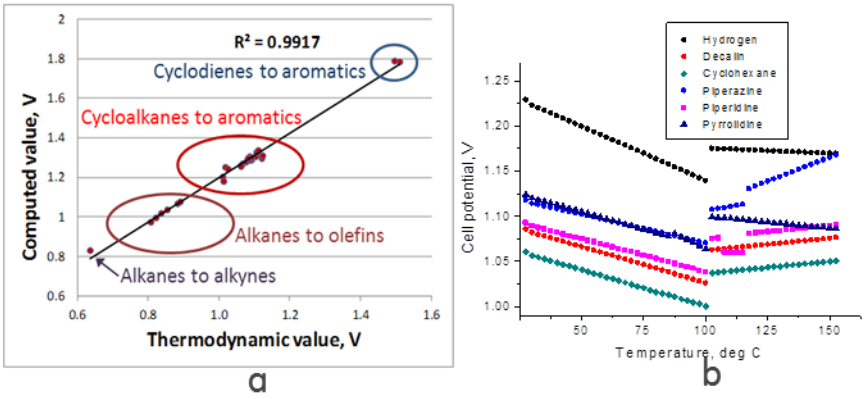

Figure 2. Computational vs. experimental cell OCP (a) and temperature dependence of OCP for model carriers (b).

SYNTHESIS OF ORGANIC FUELS

We have developed synthetic methods for preparation azaheterocycles in multi-gram scale.

Synthetic methods for selected saturated and unsaturated.heterocycles (2-alkylquinoxaline, N-alkyl-1,8-pyrrolopyridine, 9-alkyloctahydropurine) are being developed (no published synthetic routes found). The synthesis of target 9-pentyloctahydropurine is highlighted in Fig. 3. The subsequent hydrogenation of heteroaromatics to saturated heterocycles requires selection of the catalyst and reaction condition to avoid excessive hydrogenolysis of the C-N bond.

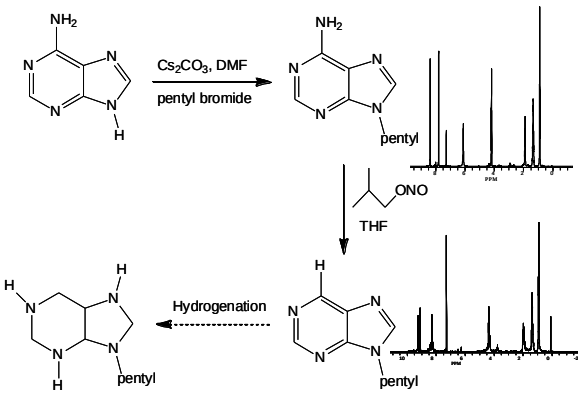

Figure 3. Synthetic strategy for synthesizing 9-pentyloctahydropurine

Modification of the hydrogen carrier fuels to anionic species could reduce interaction of basic fuels with acidic membranes and prevent their crossover through a cation exchange membrane. Nucleophilic substitution of tetrahydro-carbazole with bromo-methyl acetate allowed the preparation of anionic compounds with carboxylic or sulfonic acid side chain with a good yield.

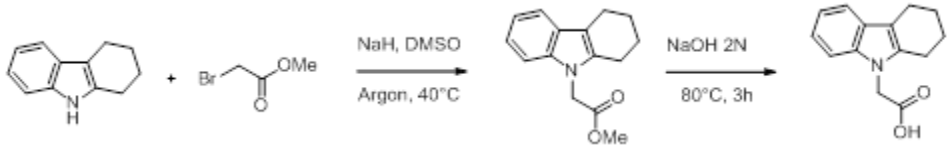

Scheme 1. Synthesis of tetrahydrocarbazole with an acidic group.

ELECTROOXIDATION OF ORGANIC HYDROGEN CARRIERS

We have discovered that fuel/base interactions can be exploited to improve oxidation kinetics.

The electrochemical oxidation of 25+ liquid organic fuels was studied. The structures of these fuels ranged from aliphatic carbocycles to a variety of heterocycles. It was found that the inclusion of

heteroatoms in the ring system of the fuel leads to a significant lowering of the subsequent oxidation potential of the fuel. There was a negative shift in the oxidation potential by more than 1 volt by the addition of a single nitrogen atom in the ring, going from tetralin to tetrahydroisoquinoline. Further reduction in the oxidation potential was achieved by moving the nitrogen atom into conjugation with the appended aromatic ring (e.g., in tetrahydroquinoline).

Modeling of measured redox potentials of substituted tetrahydroquinolines was undertaken using DFT methods in the gas phase assuming oxidation to a minus hydrogen radical (Eq. 2). The model trends well with experimental data (Fig. 4***).*** The oxidation potential of nitrogen heterocycles in which the heteroatom is conjugated to an aromatic ring can be adjusted by the introduction of substituents in the para position on the aromatic ring. The addition of a 6-methoxy group to tetrahydroquinoline leads to the greatest lowering of oxidation potential relative to methyl-, H-, methylester-, or nitro-functionality. The electron donating ability of the alkoxy group within a conjugated, aniline-like molecule, aids in stabilizing the resulting radical that is formed upon electrochemical oxidation. Hence electron donating groups ortho and/or para to the nitrogen atom in tetrahydroquinoline are expected to lower the thermodynamic barrier for oxidation. Future modeling efforts will focus on predicting absolute values of redox potentials by including condensed phase computations.

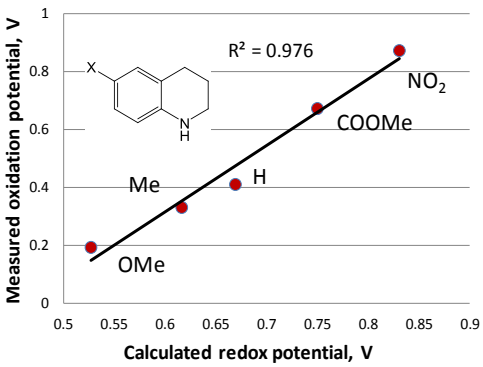

Figure 4. Substituent effects on the oxidation potential of 6-substituted tetrahydroquinolines**.**

$$2LH_n + ½\ O_2 \rightarrow LH_{n-1}^{\cdot} + H_2O \qquad (2)$$

The effect of substituents on the oxidation potential of 2- and 3-substituted piperidines with electron donating (alkyl and alkoxy) substituents is minimal. The potential only changes considerably (up to +0.36 V) when a highly electron withdrawing substituent (CF_3) is in the alpha position to the piperidine nitrogen. This is explained by the lack of pi conjugation at the nitrogen atom. It is therefore more effective to utilize a fuel that has a low barrier for electrooxidation based on the ability to stabilize a radical cationic structure. The aniline-like substructure in tetrahydroquinoline with electron donating substituents on the 6,8-positions provides likely candidates. Blocking positions on the ring that may participate in oxidative coupling reactions increases the stability of intermediate cation-radicals, for instance, in the case of 5-methoxy-N-methylindoline, which demonstrates a perfectly reversible one-electron oxidation wave while compounds with one position blocked are oxidized irreversibly (Fig. 5).

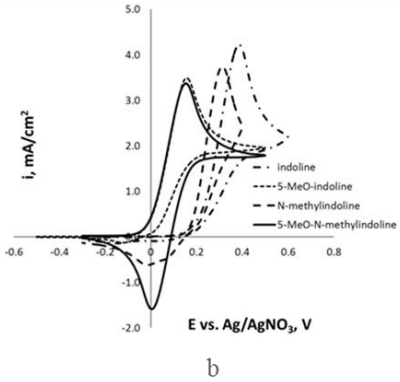

b

Figure 5. Cyclic voltammetry of substituted indolines**.**

The kinetics of liquid organic fuel electro-oxidation was further explored using rotating disk electrode (RDE) voltammetry techniques on a Pt disk. This study showed that for carbocyclic fuels the electro-oxidation does not reach the mass transport regime during the oxidation process indicating slow oxidation kinetics and possible passivation of the electrode surface. However, the N-containing heterocycles (e.g. THQ and indoline) exhibited classical RDE behavior indicating the N-atom in conjugation with the aromatic ring favors fast electron transfer. Contrarily, the RDE performance of THIQ was similar to that of carbocyclic fuels, which led to the conclusion that the presence and position

of the N-atom as well as the availability of resonance stabilization of the incipient radical cation is critical to the oxidation process. The number of electrons transferred during THQ oxidation was 2.2 and preparative electrolysis experiments further indicated that dimers and oligomers are the only soluble products detected.

We have been studying electrooxidation of fuels in the presence of a base mimicking the role of the PEM in the fuel cell. The presence of a base impacted the electrochemical oxidation of fuels when the added base was a stronger base than the fuel itself (many of the nitrogen containing liquid fuels are also basic). Two trends were discovered during these experiments. The first was that there was an increase in current for the fuel oxidation in the presence of the base. The second trend pertained to fuels that contained a nitrogen atom conjugated to an aromatic ring. In these cases, a shift of the onset of oxidation to lower potential was observed with increasing base concentration, along with the increase in current. Based on spectroscopic and electrochemical experiments, a hydrogen bonding complex was formed prior to electrochemical oxidation has been proposed for these fuels in the presence of nitrogen bases. This hypothesis was supported by a linear correlation between the shift in oxidation onset and both the base pK_a (Fig. 6) and with the energy of ionization of the hydrogen bonding complex (by DFT calculations). Preparative electrolysis experiments of indoline with a weak base such as 2,6-lutidine showed no indole formation. When a stronger base such as tetramethylguanidine (TMG) is used, electrolysis produces low yields of the desired product, indole. DFT calculations suggest that in the case of TMG, oxidation of the hydrogen bonding complex results in proton transfer to the base. The generated radical may allow for the possibility of further oxidation and deprotonation to afford indole.

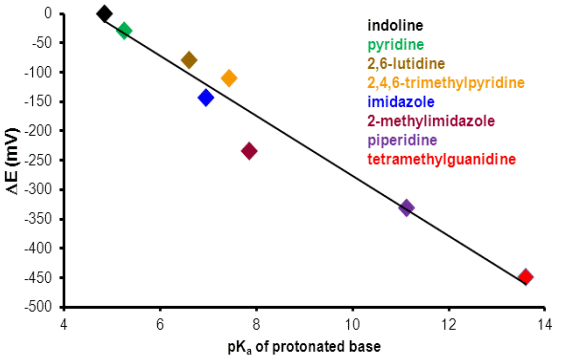

Figure 6. Oxidation onset shift as a function of the pKa of the protonated base for organic liquid fuels.

The base effect can be exploited to move the oxidation potential of the fuel to lower voltages, allowing the utilization of catalysts with lower oxidation potentials as well as enabling an increase in the power output of a fuel cell. For example, imidazole can be added to indoline to give current at a potential that overlaps with the oxidation peak of ferrocene. We also learned from our structure-property studies of catalysts that adding electron density to the ligands lowers the oxidation potential. For example, ferrocene has an oxidation peak at approximately +0.15 V whereas decamethylferrocene is oxidized at -0.4 V. By using the stronger base, tetramethylguanidine, the oxidation of indoline can be shifted to the same potential window as the oxidation peak for decamethylferrocene. An operational catalyst at this potential would allow about 1 V of output voltage.

PREDICTION AND TUNING REDOX POTENTIALS OF OUTER SPHERE ELECTROCATALYSTS

***We developed an accurate computational tool for design of outer sphere electrocatalysts with required redox potentials*.**

Several methods have been analyzed for computing redox potentials of transition metal complexes in non-aqueous solutions based on free energy density functional theory (DFT) calculations. These methods are directly compared to measured redox potentials for a series of benchmark complexes, $[MCp_2]^{0/+}$, $[MCp^*_2]^{0/+}$ and $[M(bpy)_3]^{2+/3+}$ (bpy = 2,2'-bipyridine, Cp = η^5-cyclopentadienyl, Cp* = η^5-1,2,3,4,5-pentamethylcyclo-pentadienyl; M = Fe, Co, Ni, Ru, Os, and Ir) in various non-aqueous solvents to establish the robustness of the method and the level of theory necessary for quantitative redox

potential predictions. Agreement between theory and experiment has been significantly improved relative to previous studies through the use of an appropriate (same row in the periodic table as experimental system) internal reference couple measured and calculated under the same solvent and electrolyte conditions. Our method provides accurate computation of redox potentials of transition metal complexes with a mean of -2 mV and a standard deviation of 64 mV at moderate cost (Fig. 7).

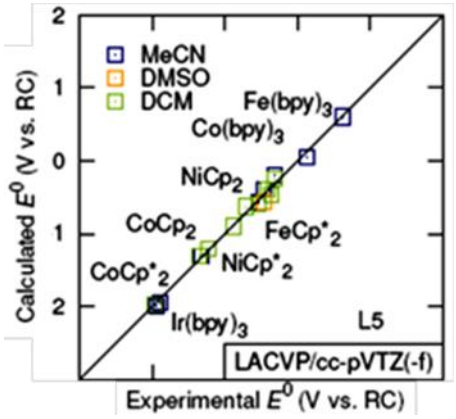

Figure 7. Correlation of measured $E_{1/2}$ and calculated $E°$ in V vs. the appropriate reference couple, RC.

For rapid outer sphere electron transfer, Marcus-Hush theory predicts that at constant driving force the change in free energy that accompanies the redox process (i.e. the difference between the redox potentials of the electrocatalyst and substrate) is limited to ca. 0.50 V. In this context and as described above, it is important to be able to tune electrocatalyst oxidation potentials to be more negative than that of the liquid fuel.

A series of substituted bis(imino)pyridine cobalt(II) chloride complexes were prepared to quantify changes in the oxidation potentials of outer-sphere electrocatalysts (left side of Scheme 2). Although the oxidation potential of these complexes varies with the electronic properties of the substituents, this method of tuning redox potentials is complicated by disproportionation leading to coordinatively saturated $[(NNN)_2Co][CoCl_4]$ salts (right of Scheme 2). Evaluation of the electrochemical properties of the analogous hexafluorophosphate salts of the $[(NNN)_2Co]^{2+}$ cations revealed a strong linear dependence of the $Co^{II/III}$ oxidation potential with the Hammett substituent parameter of the *para* substituents, with a range of 0.75 V accessible in acetonitrile. Furthermore, the oxidation potential is also significantly affected by solvent polarity, decreasing by ca. -0.60 V as solvent dielectric constant increases from ε_o = 8.9 (CH_2Cl_2) to ε_o = 80.4 (H_2O). In addition, the equilibrium shown in Scheme 7 is heavily influenced by both the solvent polarity and the steric and electronic properties of the bis(imino)pyridine ligands. In strong polar solvents (*e.g.*, CH_3CN or H_2O) or with electron donating substituents (R = OCH_3 or $N(CH_3)_2$) only oxidation of $[(NNN)_2Co][CoCl_4]$ is observed. Conversely, in nonpolar organic solvents such as CH_2Cl_2 or with electron withdrawing substituents (R = CN or CF_3), disproportionation is suppressed and oxidation of the $(NNN)CoCl_2$ species leads to solvated 18 e^- Co^{III} complexes. These results are supported by a single crystal x-ray structure of $[(NNN)_2Co][CoCl_4]$ isolated from the reaction mixture and density functional theory calculations which reproduce both the effect of ligand substituents on the $Co^{II/III}$ oxidation potentials and the thermodynamic preference for disproportionation of $(NNN)CoCl_2$ complexes in polar coordinating solvents.

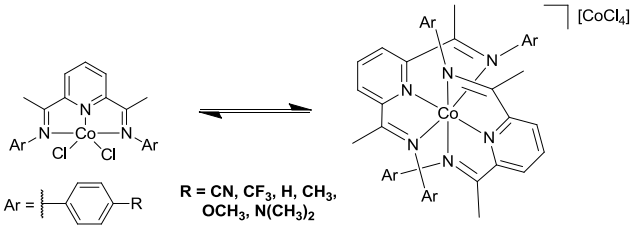

Scheme 2. Disproportionation equilibrium in solutions of NNN Co pincer chloride complexes.

This approach is not unique to these cobalt pincer complexes as a range of redox potentials is accessible from +0.09 V to -0.55 V vs. $Ag/AgNO_3$ using appropriately substituted ferrocenes. Use of a linear free energy relationship allows for rational modification of existing or design of new electrocatalysts with a desired redox potential.

OUTER SPHERE ELECTROCATALYTIC OXIDATION OF MODEL FUELS

We demonstrated that outer sphere electrocatalytic oxidation of organic carriers may be directed to dehydrogenation pathway by using a base and stabilizing intermediate radicals.

A potential fuel candidate, *N*-ethyldodeca-hydrocarbazole (NEC-H_{12}), and the major possible intermediates in its dehydrogenation to *N*-ethylcarbazole, octahydro- (NEC-H_8) and tetrahydro- (NEC-H_4) have been prepared at the tens of grams scale and studied by cyclic voltammetry. Ferrocenes catalyze NEC-H_{12} and NEC-H_8 electrooxidation to NEC in the presence of a strong base, but are inactive towards NEC-H_4 oxidation, which exhibits more positive oxidation potential (Fig. 8). These data correlate with DFT calculation of the first oxidation potentials of saturated and aromatic N-heterocycles.

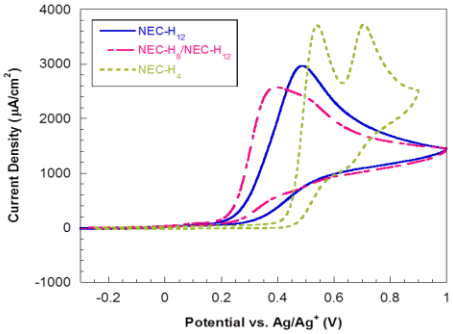

Figure 8. CVs of NEC-H_{12} (blue), NEC-H_8/NEC-H_{12} mixture (pink), and NEC-H_4 (green), 100 mV/s, 0.1 M $TEABF_4$ in MeCN.

PROOF OF PRINCIPLE-ELECTROCATALYTIC DEHYDROGENATION OF FUEL USING AN ORGANIC CATALYST

By combining the synergistic expertise of electrochemists, organometallic chemists, organic chemists and theoreticians, we have demonstrated the first example of organoelectrocatalytic dehydrogenation of a liquid fuel and elucidated the mechanistic pathway.

We have found that 2,3,-dicyano-4,5-dichloro-1,4-benzoquinone (DDQ) spontaneously dehydrogenates N-benzylaniline to yield N-phenylbenzylimine. Mechanistic insight was gleaned from computational analysis at the DFT BH&H/6-311++G9d,p) level, indicates that N-benzylaniline and DDQ form a 1:1 complex stabilized by stacking and charge transfer interactions. Approximately 0.25 e units of charge are transferred from N-benzylaniline to DDQ, yielding zwitterionic character to the complex, and a strong electrostatic attraction that brings the stacked aromatic moieties in close contact with each other. The interaction of a carbonyl moiety of DDQ with a benzyl hydrogen of N-benzylalinine leads to hydride transfer, forming a highly unstable ion pair, via a transition state in which the benzyl hydrogen bridges the N-benzylalinine and the quinone. Rotation of the deprotonated hydroquinone is almost barrierless and leads to proton transfer from the benzyl cation to the deprotonated hydroquinone providing N-phenylbenzylimine and hydroquinone. The overall dehydrogenation reaction is exothermic, releasing ~35 kcal mol^{-1}.

Experiments in which DDQ was reacted with toluene and substituted toluene to yield benzyl, 2,3-dichloro-5,6-dicyano hydroquinone or it substituted variants supported the proposed mechanism above (Eq. 3). In this case, as there is only one hydride available for transfer from the substrate (toluene) to DDQ, the pathway proceeds identically to that described above through formation of an ion pair, but the final step is bond formation between the benzyl cation and deprotonated hydroquinone. Competition experiments between toluene and substituted toluenes with substoichiometric amounts of DDQ were

performed to establish a linear free energy relationship (LFER) for the reaction. Plotting the log of the relative ratios of products for each reaction versus the σ^+ parameter for the given substituent gives a ρ^+ value of -3.28, consistent with a considerable build-up of positive charge in the rate determining transition state for this reaction (Fig. 9).

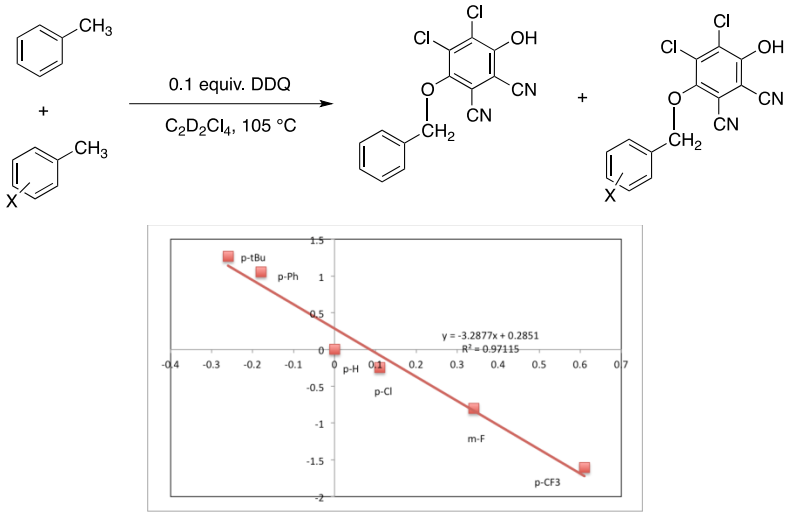

(3)

Figure 9. Hammett plot of the reaction of substituted toluenes with DDQ

To further probe the nature of this mechanism, intermolecular deuterium kinetic isotope effects were determined through competition experiments of toluene and d_8-toluene revealing a k_H/k_D of 5.2 (Eq. 4), consistent with breaking of the C-H bond in the rate-determining transition state. This result coupled with the large negative ρ^+ value from the LFER, strongly suggests that the reaction proceeds *via* hydride abstraction from toluene by DDQ.

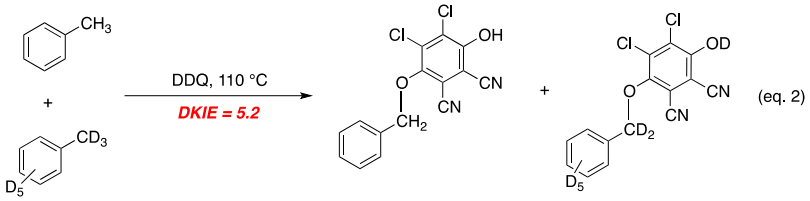

(4)

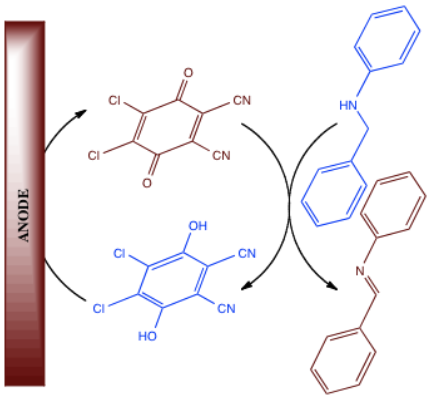

In order to complete the catalytic cycle, DDQ must be regenerated from the hydroquinone. We have found that electrolysis at 0.96 V vs. NHE allows DDQ regeneration from the hydroquinone (which forms immediately after addition of quinone to the substrate). In a controlled potential electrolysis experiment, we obtain 95% conversion of N-benzylalinine to N-phenylbenzylimine after 6 hours. This is the first case of DDQ being employed as a mediator in an electrocatalytic dehydrogenative process (Fig. 10).

Figure 10. DDQ mediated dehydrogenation of N-benzylaniline

The effect of base on the electrochemical regeneration of DDQ has been determined (Fig. 11). As is the case in the uncatalyzed oxidation of fuels in the presence of base, the base functions as a proton sink, driving the equilibrium towards the dehydrogenated species. Large catalytic currents are seen in the cyclic voltammograms of solutions where lutidine has been added to the reaction product of DDQ. In the absence of lutidine, catalytic currents are also seen at high concentrations of benzylaniline which can act as a base when in stoichiometric excess. Interestingly, at low concentrations of benzylaniline, addition of base also results in catalytic currents, indicating again that the base can drive the equilibrium toward the dehydrogenated DDQ even at near stoichiometric ratios of the starting materials.

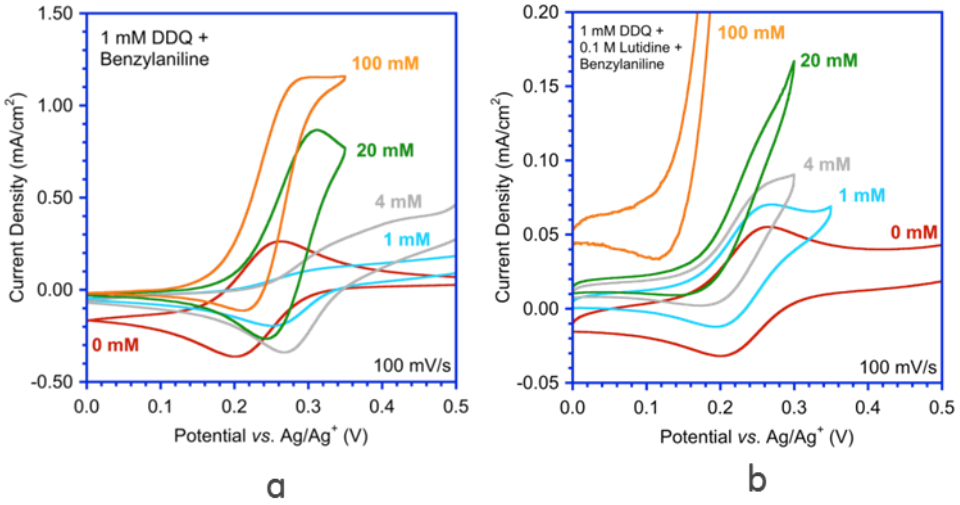

Figure 11. Cyclic voltammograms of DDQ and N-benzylaniline without base (a) and with base(b).

ELECTROCATALYTIC DEHYDROGENATION AND HYDROGENATION OF NITROGEN HETEROCYCLIC FUELS USING FIRST ROW TRANSITION METAL COMPLEXES WITH NON-INNOCENT LIGANDS

Using ligands active in proton and electron transfer we have demonstrated electrocatalytic dehydrogenation and hydrogenation of liquid fuels with first row transition metal complexes.

Electrodehydrogenation of a N-heterocycle using nickel complexes with redox-active ligands. Redox-active water- and air-stable complex **1** (scheme 3) has been shown to act as an operationally homogeneous catalyst for the electrodehydrogenation of the saturated N-heterocyclic substrate, 1,2,3,4-tetrahydroquinaldine to give the corresponding arene. Cyclic voltammograms of compound **1** in the presence of incremental additions of this substrate show a sharp increase in current response, characteristic of a catalytic process (Fig. 12). As derivatives of anilines often show polyaniline-forming side-reactions, the isolated yields of the desired fully unsaturated product were compared with accumulated charge. The reaction was shown to occur in 70-90% faradaic yield with 78% chemical isolated yield. A series of water and air stable organometallic CpNi N-heterocyclic carbene complexes with highly donating ligands were synthesized by the direct reaction of the azolium salt with Cp_2Ni. These compounds did not show catalytic activity in the electrodehydrogenation reaction. However, addition of a free quinone to an otherwise electrocatalytically unreactive non-quinoid CpNi NHC complex **2** exhibited electrocatalytic behavior, although not as active as in the case of **1**.

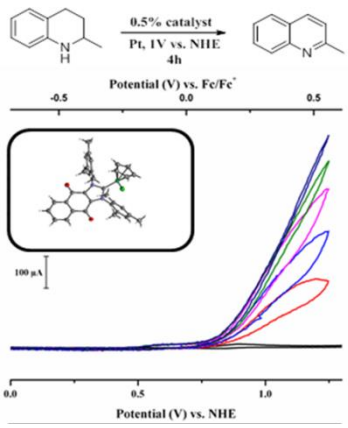

Figure 12. Electrocatalytic dehydrogenation of 1,2,3,4- tetrahydroqinaldine.

Scheme 3. Synthesis of CpNi N-heterocyclic carbene complexes with quinoid moiety,

Electrochemical reduction catalyzed by nickel complexes with basic ligands. We have studied low-coordinate tridentate NNN nickel pincer complexes with various placements of basic centers in the ligand to understand the mechanism of formation of hydride equivalents. The ultimate goal of the study is the interception of such equivalents in the process of reduction of a spent fuel molecule. These complexes hydrogenate organic aromatic substrates and reduce protons at low overpotential (up to 140 mV). We optimized the catalyst design starting from catalyst **3,** which is active in mixed aqueous/acetonitrile media, to a redox-active ligand motif in a water-soluble, highly-conjugated NNN pincer **4** which is electrocatalytically active in highly acidic media (pH <3). Addition of multiple basic sites shifted the working pH region to almost neutral for complex **6**. This compound was capable of electrocatalytic hydrogenation of 2,3-dimethylquinoxaline with an isolated yield of 42%. Computations suggest an initial ligand reduction followed by proton-coupled electron transfer to give the catalytically active Ni(II)-H species.

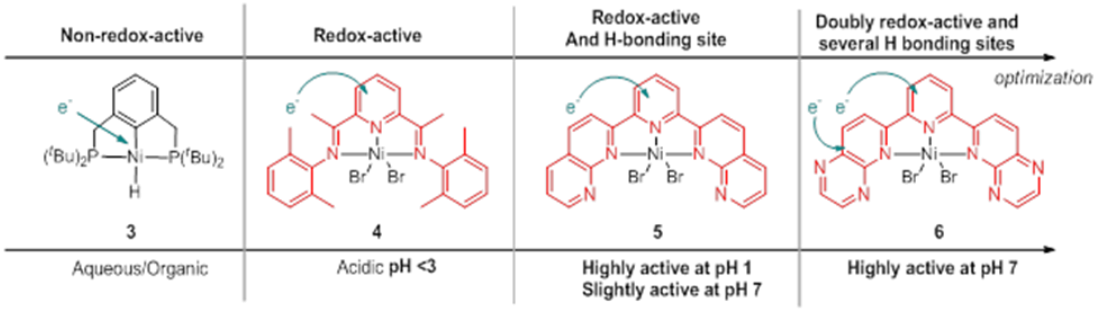

Combining temperature-dependent paramagnetic ^{1}H NMR and DFT methods, we have assigned all protons in paramagnetic NNN Ni^{II} complexes. This approach is extremely valuable in the search of appropriate ligands to optimize the reactivity of 3d metal complexes.

Mechanistic study of reduction of both proton and nitrogen heterocyclic compounds in water catalyzed by NNN Ni complexes showed that N-donor chelating ligands are redox active. A Ni^{II} hydride is involved in proton reduction and the proposed catalytic cycle (left of Fig. 13) has been analyzed computationally using the DFT B3LYP/cc-pVTZ level of theory. This cycle includes redox transformations of both the metal center and the bis(imino)pyridine ligand allowing a net $2e^{-}/2H^{+}$ transformation. The computed reaction free energy profile (right of Fig. 13) shows that proton coupled electron transfer (PCET) enables transformation of $[1'(OH2)]^{+}$ into $[1'(H)]^{+}$ at low voltage. An alternative reaction pathway involving conversion of $[1'(OH2)]^{+}$ to $[1'(H)]^{+}$ via sequential protonation and reduction without invoking PCET is thermodynamically unfavorable.

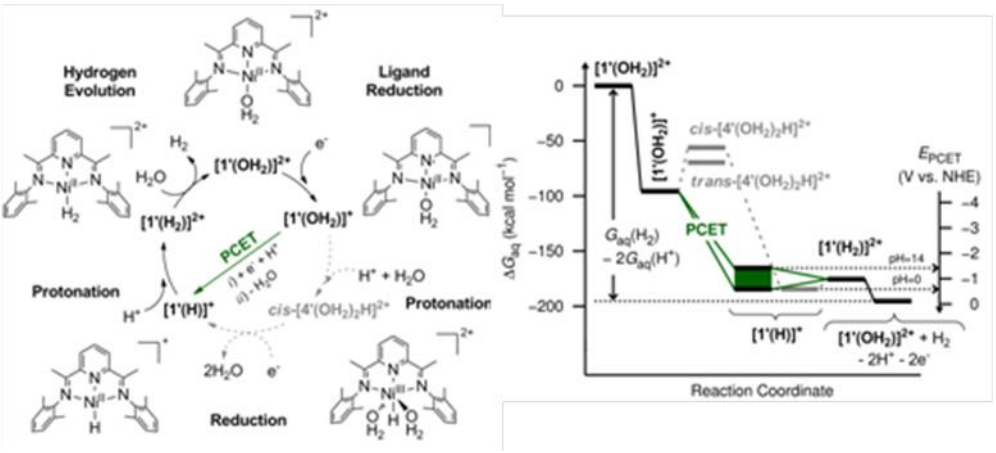

Figure 13. Proposed catalytic cycle for hydrogen evolution based on $(NNN_{Me})Ni(OH_2)^{2+}$ (left) and the corresponding computed reaction free energy profile (right).

Two series of nickel-based complexes with tunable electronic and steric properties were synthesized employing chelating ligands (bisphosphinite or POCOP ligands) and tris(pyrazolyl)borate ligands (Tp and Tp') (Scheme 4). (POCOP)NiCl and (POCOP)NiH complexes are electrochemically well-behaved and they show reversible $Ni^{II/III}$ redox processes in acetonitrile. Electron-donating or –withdrawing substituents at the para position of the aromatic ring of the ligand allowed tuning of the oxidation potential.

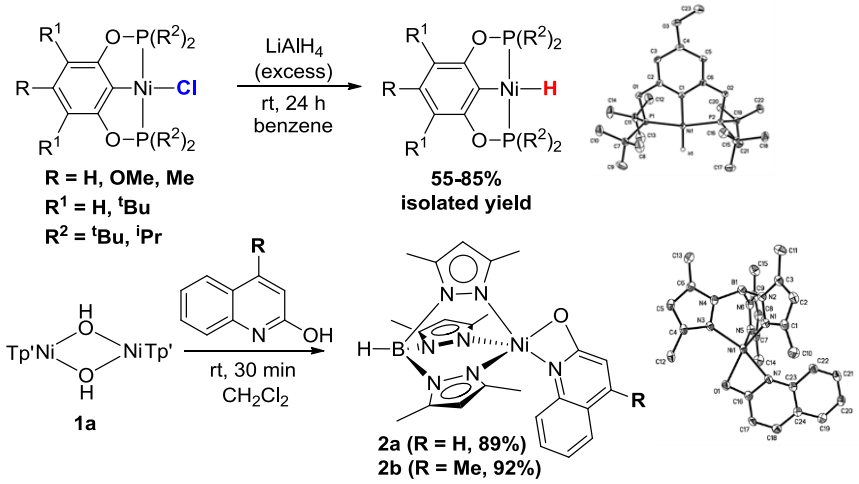

Scheme 4. Synthesis of (POCOP)Ni and Tp'Ni complexes.

FUNDAMENTAL UNDERSTANDING OF ELECTROCHEMICAL PROPERTIES OF METAL HYDRIDES

Using a combination of theory and experiments we have developed a fundamental understanding of factors controlling redox properties and acidity/hydricity of the M-H bond on rhodium hydride complexes.

In order to understand the mechanism of electrochemical dehydrogenation, we studied competitive reactions of deprotonation of and H_2 generation from the Rh(III) hydride generated according to the catalytic cycle depicted here. Though spectroscopically observed Rh-H species **4** as well as the unstable Rh(I) species **2d** were not isolated, the proposed mechanism (Scheme 5) was consistent with the electrochemical properties of complexes with various ligands (**a** – **d**) and theoretical computations. In MeCN, reduction of **1a-c** were chemically reversible and are in agreement with a metal-centered, two-electron reduction to the Rh(I) complexes **2a-c** while reduction of **1d** was irreversible. Complexes **2a** and

2b were isolated from reduction of Cp*Rh(chelate)Cl_2 with excess KC_8. X-ray structure and geometry calculations showed that coordination of ligand **d** is different from **a** – **c** which leads to energetically favored displacement of this chelating ligand with two MeCN molecules from **2d** (-2.6 kcal/mol vs. 15.4 kcal/mol for **2a**). Thus, the computational results are consistent with the experimental CV data.

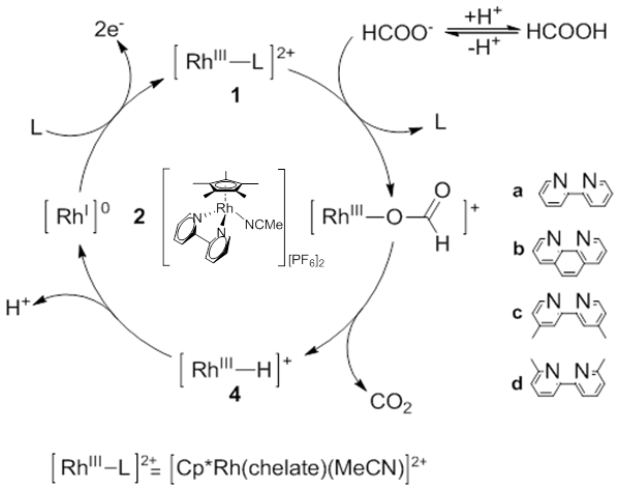

Scheme 5. Catalytic cycle for electro-dehydrogenation of formate with catalyst [Cp*Rh(bpy)(MeCN)][PF_6]$_2$.

Upon addition of formate to a MeCN solution of complexes **1a-c**, the redox potentials shifted in the cathodic direction, indicative of coordination of the more electron-rich formate ligand. This was confirmed by isolation of more stable acetate analogues. It was found that electrocatalytic activity of **1** in MeCN quickly diminished due to decomposition. Replacement of MeCN with less coordinative PhCN resulted in electrocatalytic activity of **1a-b** in the formate dehydrogenation with a 78% yield. The catalyst remained active with subsequent additions of the substrate.

Utilization of DFT calculations showed how to further tune the ligand set to improve the acidity vs. hydricity of the metal center. Calculating the protonation of complexes **4** by proton sponge-H^+ versus deprotonation by proton sponge has allowed for a metric for comparing relative acidities and hydricities. Hydricities increase in the order a<b<c<d; opposite the order of the acidities (Fig. 14). From these computations, it's been shown that the relative acidity of complexes decreased with the increasing electron donating ability of the chelating ligand. Using combined experimental and theoretical approaches we probed reactivity of non-isolable intermediates and identified a ligand set that would promote the desired M-H acidity and thus favor the targeted electrocatalytic cycle. It should be noted that the rhodium catalyst is regenerated at potentials that are greater than one volt more negative of where substrate is oxidized at the electrode. This demonstrates the use of inner sphere catalysis to optimize for energy generation.

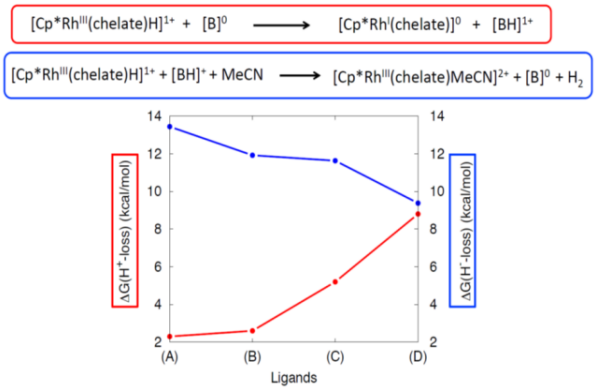

Figure 14. Relative hydricities and acidities of complexes

We utilized formate as a hydride source in the catalytic cycle shown in Scheme 5 to access the Rh hydride and study its electrochemical properties. This catalyst, [Cp*Rh(bpy)(MeCN)][PF_6]$_2$, can electro-catalytically oxidize formate at a notably low potential of -0.9 V vs. Ag/Ag^+. With 20 mM formate and 2 mM of the Rh electrocatalyst, a maximum faradaic efficiency of 67% was observed with the electrode solution still active towards electrocatalytic oxidation of further aliquots of formate. The proposed catalytic cycle (scheme 4) was elucidated by identification of all intermediates: reduced Rh(I) species (isolated), Rh-H (observed by NMR), and Rh-OC(H)O (modelled with Rh-OAc species).

[Cp*Rh(bpy)(MeCN)][PF_6]$_2$ turned out to be inactive in electrooxidation of a variety of hydrogenated heterocycles (1,2,3,4-Tetrahydroquinoline, *N*-benzylaniline, 1,2,3,4-tetrahydrocarbazole, and 5-amino-

1,2,3,4-tetrahydroisoquinoline) indicating the high barrier to forming the Rh(III) hydride from these species. 1,2,3,4-tetrahydroisoquinoline (THIQ) which features a weaker benzylic proton adjacent to the amine functionality can be electrodehydrogenated under moderately elevated temperatures of 80°C at the electrocatalyst's redox potential to 3,4-dihydroisoquinoline and quinoline.

LIGAND ASSISTED SEPARATION OF ELECTRON AND PROTON TRANSPORT AND ELECTRODEHYDROGENATION OF OXYGENATED FUELS ON IRIDIUM COMPLEXES

Using iridium complexes with non-innocent ligands, we have demonstrated chemical and electrochemical separation of electron and proton transfer and microscopic reversibility.

Our work with Ir-based dehydrogenation electrocatalysts $[Ir(trop_2DACH)]^+$ and $[Ir(trop_2DAD)]^+$ continued with efforts focused on (a) gaining an understanding of catalyst activation and possible electrocatalysis mechanism, and (b) electrolysis reproducibility using a new preparative cell design to identify critical variables (e.g., solvent coordination properties and base strength) to maximize Faradaic efficiency and electrochemical yield.

Electrocatalyst activation under basic oxidative conditions. An open question we had with $[Ir(trop_2DACH)]^+$ was whether the starting complex underwent stepwise proton and electron loss to 'end' at a mono-deprotonated and mono-oxidized ('active') radical cation, $[Ir(trop_2DACH_{-1H})]^+$ (**2**$^+$ in Scheme 6), or if it was possible for $[Ir(trop_2DACH)]^+$ to undergo multiple proton and electron loss under electrolysis conditions. Based on a combination of ^{1}H NMR spectroscopy, cyclic voltammetry and thermochemical calculations we proposed a mechanism for catalyst activation (Scheme 6). The starting complex **1** undergoes two proton and two electron loss to engender the formation of a doubly deprotonated-doubly oxidized species, diiminocyclohexane based **4,** through the intermediacy of the mono-imino-mono-aminocyclohexane complex **5** under basic electrolysis conditions. Based on the literature pKa1 of $[Ir(trop_2DACH)]^+$ (close to 10.5) and the measured redox potential of the mono-deprotonated complex at $E_{½}$ = -0.21 V vs $Fc^{+/0}$ we calculated that a homolytic bond dissociation energy (H-atom removal) at this step required 79.2 kcal/mol. A second deprotonation is more facile given a computed pKa2 of 9.2. We observe a second oxidation (E_{PA} = -0.2 V vs. $Fc^{+/0}$) to substantiate double-deprotonation and oxidation as a necessary activation step required for the catalyst to perform electrooxidation of primary alcohols.

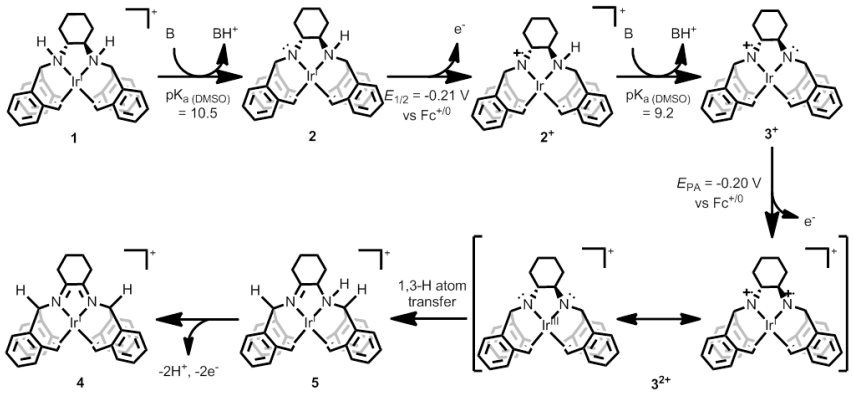

Scheme 6. Proposed mechanism for in situ conversion of 1 to 4 based on NMR spectroscopy, cyclic voltammetry and thermochemical calculations.

Steps involved in the conversion of **1** to **5** (Scheme 6) are based upon experimentally determined or calculated redox potentials and pK_a values of **1**, **2**, **2**$^+$ and **3**$^+$ (in DMSO) as well as the results of ^{1}H NMR experiments showing the formation of **4** and **5** upon oxidation of **3** with silver(I). Electrolysis results have shown not only that **4** is catalytically competent in the electrocatalytic oxidation of 4-methoxybenzyl alcohol to *p*-anisaldehyde but that it performs as well as **1**.

Bulk electrolysis: Identifying parameter sensitivities. We developed a new cell design, with a Pt gauze placed directly next to the glass frit on each side of the cell, which minimized run-to-run variability and established reproducibility. Critical variables for bulk electrolysis of 4-methoxybenzyl alcohol using $[Ir(trop_2DACH)]^+$ in conjunction with sodium 4-nonylphenolate have been identified, e.g., a solvent effect of coordinating and non-coordinating solvents. For example, THF allowed for high isolated yield of p-anisaldehyde, however Faradaic efficiency was moderate (73%). When acetonitrile was employed, no electrooxidation was observed. Non-coordinating solvents such as o-dichlorobenzene and o-difluorobenzene (o-DFB) both provided high Faradaic efficiencies (>95%), but o-DFB showed the best yield. We also observed a base effect after a number of p-substituted (sodium and tetrabutylammonium) phenolate bases were screened in o-DFB.

Isolated yield of p-anisaldehyde almost doubled when sodium p-chlorophenolate was used in lieu of sodium 4-nonyl phenolate over the same period of time at the same low applied oxidation potential (without loss of Faradaic efficiency). Shifting away from phenolates to other bases, we observed the highest Faradaic efficiency to date (100%) with tetrabutylammonium 4-cyanobenzoate (with decent yield), and the highest p-anisaldehyde yield to date using guanidine (with 95% Faradaic efficiency). Both of these non-phenolate bases, including sodium 4-chlorophenolate, will be tested for performance with other catalysts $[Ir(trop_2DAD)]^+$ and it's cyclohexyl version $[Ir(trop_2DICH)]^+$.

MICROREVERSIBILITY OF CATALYTIC DEHYDROGENATION (with NYSTAR funding)

Using iron hydride complexes with similar ligand environments, we have demonstrated microreversibility of catalytic dehydrogenation of nitrogen heterocycles with a first row transition metal catalyst.

An iron PNP pincer complex has been found to catalytically dehydrogenate tetrahydroquinolines, tetrahydroisoquinolines, dihydroindoles, and piperidines (Scheme 7, a). These reactions occur thermally in refluxing xylene, where the thermodynamically unfavorable reaction can be driven uphill. The reverse reaction, hydrogenation of quinolines, can be catalyzed by (PNP)FeHBr using 5-10 atm H_2 at 80 °C (Scheme 7, b). Dehydrogenation of secondary alcohols can also be driven to form ketones with as little as 0.1% catalyst.

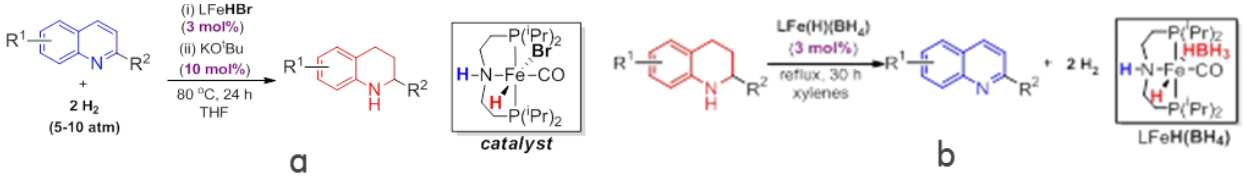

Scheme 7. Hydrogenation (a) and dehydrogenation (b) of N-heterocycles in the presence PNP Fe complexes $[Cp^*Rh(bpy)(MeCN)][PF_6]_2$.

To drive a dehydrogenation reaction toward separate generation of protons and electrons requires a stoichiometric oxidant combined with a weak base as a proton sink, and for the reverse reaction (catalytic hydrogenation) a stoichiometric amount of reductant is necessary combined with a (weak) conjugate acid as a proton source. Herein, we studied two iridium(I) complexes [Ir(trop$_2$DACH)][OTf], a highly efficient catalyst used in the dehydrogenation of a broad range of primary alcohols to aldehydes, and the related [Ir(trop$_2$DAD)][OTf] that features an unsaturated and sterically less encumbered ligand framework, as reversible alcohol dehydrogenation-hydrogenation catalysts (Scheme 8).

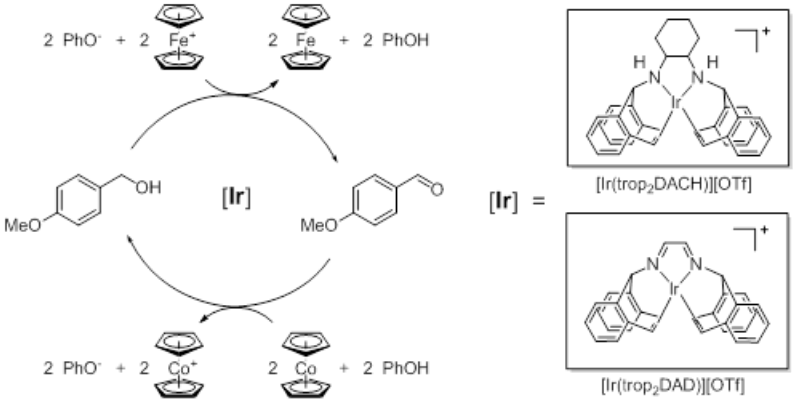

Scheme 8. Reversible oxidative dehydrogenation of 4-methoxybenzyl alcohol catalyzed by complexes [Ir(trop$_2$DACH)][OTf] and [Ir(trop$_2$DAD)][OTf]

For oxidative dehydrogenation, we employed phenolate anion as a base (proton sink) in combination with various chemical oxidants. Dehydrogenation of 4-methoxybenzyl alcohol at room temperature with 0.01 - 0.03 mol% catalyst (2 equivalents each of phenolate and oxidant relative to 4-methoxybenzyl alcohol were used) resulted in high yields (63 – 94%) of p-anisaldehyde. All working oxidants had redox potentials greater than -0.13V vs. the ferrocenium/ferrocene couple in o-dichlorobenzene, which is the peak oxidation potential (observed to be pseudo-reversible at scan rates ≥1 V/s) for mono-deprotonated catalyst, the neutral Ir-amido-amine complex [Ir(trop$_2$DACH$_{-1H}$)]^0**.** Noteworthy, by separating proton and electron transfer events in 4-methoxybenzyl alcohol dehydrogenation, no penalties were observed in terms of reaction rate or percent conversion to aldehyde relative to the concerted process with benzoquinone as an oxidant/base.

The reverse reaction, catalytic hydrogenation of p-anisaldehyde to 4-methoxybenzyl alcohol, was done using the same catalysts combined with phenol as a proton source and stoichiometric reductants. It was necessary to run hydrogenations with excess phenol ('acid') because of formation of large amounts of a precipitate, which was identified by ^{1}H NMR, CV, HPLC-TOF/MS, and TGA-FTIR as an adduct of cobaltocenium phenolate with phenol ([CoCp$_2$][OPh]·HOPh. Therefore, hydrogenation reactions were carried out with 1 mol% of the catalysts and 5 eq of phenol and 2.5 eq of reductant relative to p-anisaldehyde to achieve high yields (up to 89%). Only reductants strong enough to activate (reduce) [Ir(trop$_2$DACH)][OTf] and [Ir(trop$_2$DAD)][OTf] by one and two electrons, respectively, were able to reductively hydrogenate p-anisaldehyde. Formation of metallo-radical [Ir(trop$_2$DACH)] occurs at the peak potential -1.36V vs. Fc$^{+/0}$ correlates with activity of [CoCp$_2$], [Co(η^5-C$_5$H$_4$Et)$_2$], and [CoCp*$_2$] and inactivity of [FeCp*$_2$] and [Cr(η^6-C$_6$H$_{6)2}$.

INVERSE DESIGN COMPUTATIONAL METHODOLOGY

Inverse design methodology was demonstrated to be suitable in the optimization of catalytic cycles.

We developed an algorithm, which efficiently searches for catalyst candidate structures that minimize energy differences between related chemical structures such as reaction energies or barriers through continuous variation of *alchemical* structures in the vicinity of a reference catalyst framework. To illustrate the advantages of such a treatment and to critically review its limitations, we use our method

to optimize the catalytic activity of a Ni(II)-iminothiolate complex in a CO/CO_2 conversion cycle (Fig. 15). This nickel complex was first proposed and studied by Crabtree and co-workers as a functional model for CO dehydroxygenase. Based on the DFT analysis of possible intermediates and transition states we propose a catalytic mechanism that is in-line with available experimental data. We use the developed algorithm to identify possible trial catalysts which minimize the reaction energy of the oxidation step. DFT analysis of the resulting cycle suggests that the catalyst proposed by inverse design indeed reduces the reaction energy of the oxidation step without causing qualitative changes to the other steps involved in the cycle. The findings demonstrate that the inverse design approach can be used to tune specific reactivities in existing catalyst frameworks, making it a valuable tool for catalyst design.

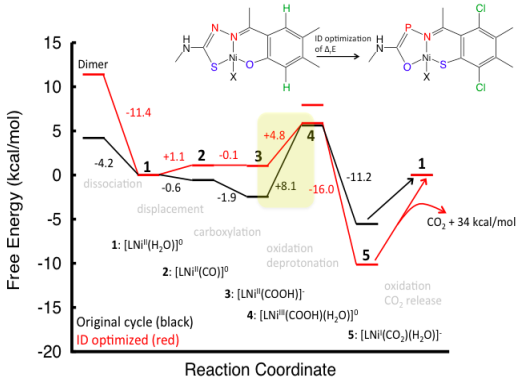

Figure 15. Illustration of the inverse design methodology applied to the Ni-catalysts for CO/CO_2 conversion.

SELECTION OF MEMBRANES FOR ORGANIC FUEL CELLS

We have analyzed suitability of different polymer backbones for organic fuel cells using solubility parameters theory.

Solubility parameters analysis. Commercial and experimental membrane materials have been considered as starting backbones: perfluorosulfonate polymers such as Nafion® and Aquivion® resins, polybenzimidazole resins imbibed with phosphoric acid, and sulfonated polyethers such as perfluorosulfonated polyarylethers and sulfonated polysulfone. Analysis of the fuel interaction with the polymer membrane and electrolyte was performed using polymer solubility parameters calculated from Askadskii QSPRs and Hansen solubility theory (Fig. 16).

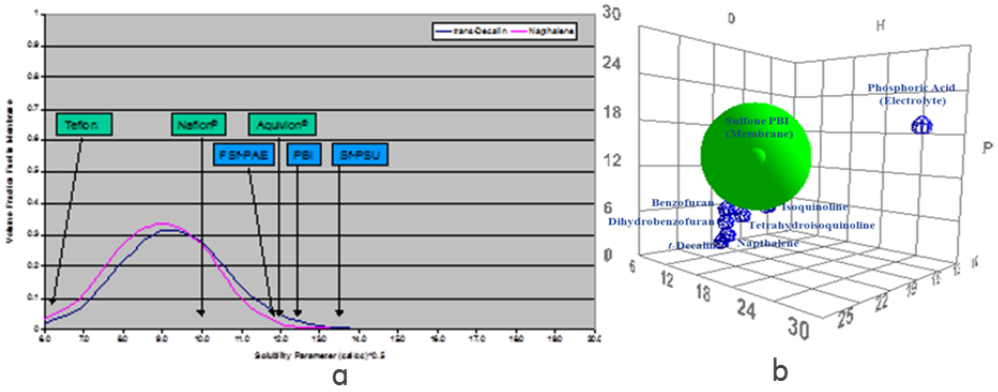

Figure 16. Calculated volume fraction fuel absorbed into 30% crosslinked polymer membrane as a function of polymer solubility parameter (a) and Hansen solubility diagram depicting various model fuels with Sulfone-PBI (R=7 $MPa^{0.5}$) membrane and phosphoric acid electrolyte (b).

Using this approach, we calculated the solubility parameters and interaction radii for a number of polymer membranes, fuels and electrolytes. Since, Hansen theory predicts fuels furthest in solubility space from the polymer membrane's solubility sphere exhibit the least favorable thermodynamic

interactions, it provided a valuable tool for identifying the most resistant polymer-electrolyte combinations for a given fuel. The analysis suggests that PEMs most resistant to organic fuel crossover should be those with higher solubility parameters than Nafion® (Fig. 16a).

Such analysis, shown in Figure 16b, identified basic nitrogen-containing aromatic membranes, such as polypyridines and polybenzimidazoles imbibed with acidic electrolytes as ideal candidates. Further optimization of the polymer's molecular structure using Askadskii/ Hansen modeling identified the novel electron-deficient poly ((6-phenylsulfonyl) benzimidazole) s (PPSBI) as an ideal candidate having excellent chemical, mechanical and oxidative stability. For the electrolyte phase, phosphoric acid demonstrated the best balance of thermal-oxidative stability and conductivity at elevated temperatures based on literature reports.

ANHYDROUS PROTON CONDUCTING MEMBRANES

We investigated microstructure of polybenzimidazole membrane materials and proposed new monomer providing enhanced oxidative stability.

We investigated polybenzimidazole as a potential membrane material with the ideal mechanical, thermal and thermal oxidative stability required for fuel cells operating at elevated temperatures; temperatures thought necessary for dehydrogenation of the most promising organic fuels. Our efforts led us in two concurrent directions. First was to develop novel high temperature polybenzimidazoles and membranes including those based on structure **1** (Scheme 9). A novel monomer was synthesized, polymerized by standard techniques (polyphosphoric acid, 200-220 ^{o}C) and the isolated polymer cast into thin film membranes from DMSO. The membranes, imbibed with phosphoric acid, exhibited high acid doping levels (H_3PO_4:benzimidazole) relative to commercial *m*-PBI (**2**) and AB-PBI (**3**) membranes and expectedly activation energies of (20.9 KJ/mol) for proton conduction than **2** and **3** (26.5 and 27.4 KJ/mol respectively). Phosphoric acid electrolyte membranes derived from **1-3** (Scheme 9) were all ca. 9x improvement in proton conductivity relative to Nafion® membranes at low relative humidity (20-60%).

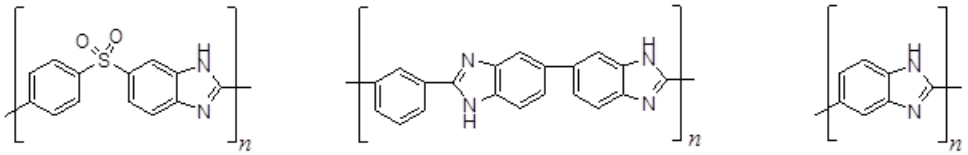

1 **2** **3**

Scheme 9. Repeated unit of polybenzimidazole polymers for proton conducting membrane backbones

Anomalies observed during NMR analysis of **1** led us to apply our learnings to a detailed structural analysis of **2** (in collaboration with Danish Power Systems). This work was important in understanding the polymer structure and polymerization chemistry, since it was recognized that high m-PBI molecular weights were an contributing factors in membrane oxidative stability, which became comparative to Nafion® for 83 kDa molecular weight, and in fuel cell performance (Figure 17a). This work provided important understandings of *m*-PBI endgroup structure wherein carboxyl, aniline and 2-*H* benzimidazole endgroups were resolved by ^{1}H-NMR spectroscopy. These endgroups were a result of 4,4'-tetraminobenzidine monomer byproducts formed during the commercial synthetic process (acetylation/nitration/reduction of 4,4'-diaminobenzidine) and incorporated during polymerization. These impurities affect stoichiometry and produce endgroups with low reactivity to polymerization. The presence of both aniline endgroups and benzanilide backbone residues formed by condensation (ca. 10:1 molar ratio) is a reflection of this low polymerization reactivity. However the presence of low levels of benzanilide groups in the polymer indicates a previously unknown source of polymer membrane

instability. The detailed ^{1}H-NMR microstructural analysis also enabled a new NMR technique for molecular weight determination (Fig. 17b), supplementing currently used viscometric methods. Its use allowed us to follow *m*-PBIs of various molecular weights during polymerization and indicated at high molecular weights a second, yet to be fully evaluated, molecular weight building process is occurring.

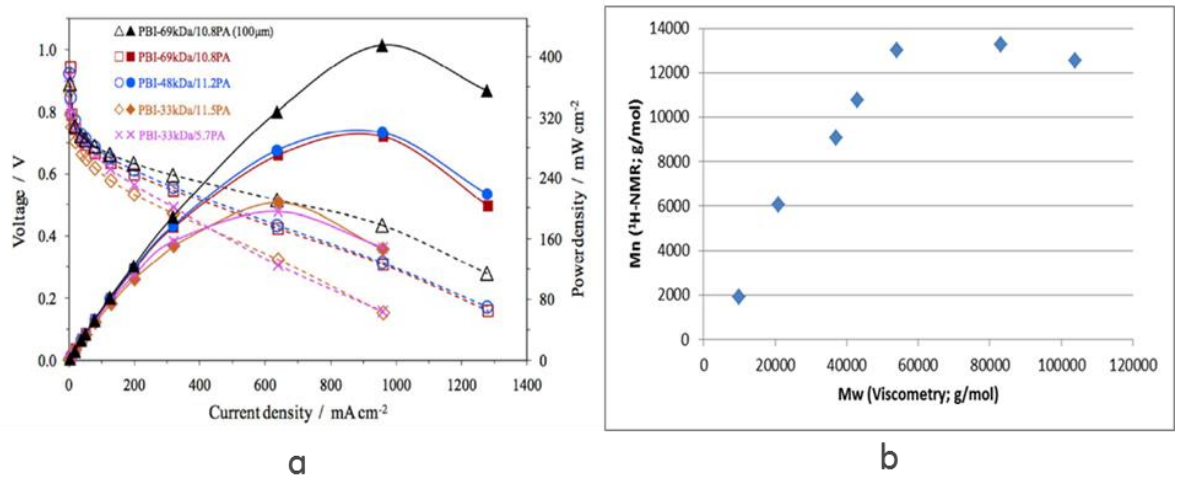

Figure 17. m-PBI MEA fuel cell performance as a function of membrane molecular weight (a) and correlation of NMR and viscosimetry data on PBI molecular weight (b).

ENHANCED PERFORMANCE OF ACIDIC PROTON EXCHANGE MEMBRANES IN THE PRESENCE OF CARBOCYCLIC PLASTISIZERS

We have demonstrated enhanced performance of fuel treated PEMs and elucidated the fuel effect on membrane morphology using SAXS and NMR.

To investigate the impact of organic fuels on hydrogen fuel cell performance, commercial Nafion® membranes were imbibed with three model fuels: decalin, dihydrobenzofuran and tetrahydroisoquinoline.

Improved water uptake and proton conductivity. Decalin treated Nafion®N212 exhibited up to a 40% increase in water uptake and 20% increase in proton conductivity. The dihydrobenzofuran treatment showed minimal changes in both suggesting these fuels can be used with existing Nafion® membrane technology with suitable electrocatalysts for fuel dehydrogenation. The treatment of N212 with N-ethylcarbazole did not show a significant decrease in conductivity while with the more basic indoline an 80% reduction in water uptake and conductivity was observed due to the formation of an acid-base complex with the sulfonic acid groups, rendering these membranes unusable with strongly basic N-heterocyclic fuels.

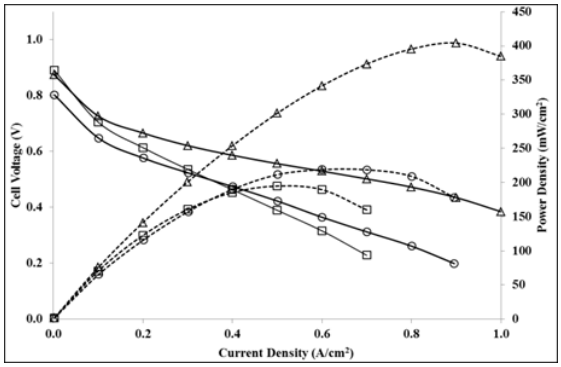

Figure 18. I-V curve (solid line) and power density (dashed line) of H_2/Air fuel cells with untreated (o), decalin treated (Δ) and DHBF treated (□) N212 at 70 ^{o}C at 60 % RH.

Enhanced fuel cell performance. The fuel cell performance of membranes doped with these fuels is shown in Fig. 18 including the undoped Nafion® 212 membrane. Decalin and dihydrobenzfuran doped MEAs did not suffer mass transport losses at

higher currents and resulted in lower H_2 crossover currents than the undoped membrane during operation. In contrast, the membranes doped with tetrahydro-isoquinoline did not produce current in the fuel cell and exhibited a large interfacial resistance. This can be attributed to basicity of tetrahydroisoquinoline, which is known to readily form salts with conductive acidic electrolytes such as sulfonic acid. Alternatively decalin and dihydrobenzofuran may provide an ideal balance of hydrophobicity and low basicity.

The decalin treated membranes showed no significant changes in performance at 100% RH when tested in a H_2/Air fuel cell suggesting no adverse physical or chemical interactions due to fuel treatment. However, at 60% RH, a profound increase in peak power density (86%) was observed for the decalin treated membranes. The decalin treated N212 exhibited a 60% reduction in hydrogen crossover along with a two-fold reduction in internal resistance that do not significantly change with reducing RH until very low values. The observed improvement in performance remained unchanged after operating the cells under steady state conditions for three days. The dihydrobenzofuran membranes did not show any changes in performance but lower hydrogen crossover and internal resistance was still observed at 60% RH in a fuel cell (Fig. 18).

Membrane morphology changes in the presence of fuels. Decalin sorption data and Hansen solubility theory predictions indicate that decalin is absorbed into the hydrophobic phase of N212. Evaluation of membrane morphology by SAXS further demonstrated that decalin suppresses crystallization of the hydrophobic phase (Fig. 19). Water uptake results revealed the greater propensity of decalin treated N212 to absorb water relative to untreated N212, consistent with reduced elastic modulus producing a lower counteracting pressure to the osmotic pressure from the sulfonate residue solvation.

Using the dependence of conductivity vs. water uptake found for Nafion® membranes in the literature, the higher water uptake values for decalin treated membranes should translate to a 4-fold increase in proton conductivity compared to untreated N212, however this was not observed. Therefore, the proton conduction in decalin treated membranes does not bear a typical relationship to water activity and could relate to a complex interaction of hydrophobic and ionic phase microstructure as evidenced by SAXS data. Despite the modest improvement in conductivity, the combined effect of membrane treatment on fuel cell performance, at low RH, is substantial. The low resistance of fuel treated membranes correlates with increased number density of the ionic domains, the size of which remains unchanged with changes in RH, and low hydrogen crossover reflects changes in crystallinity of the hydrophobic phase. Both low hydrogen crossover and resistance contribute to the substantially high power density observed

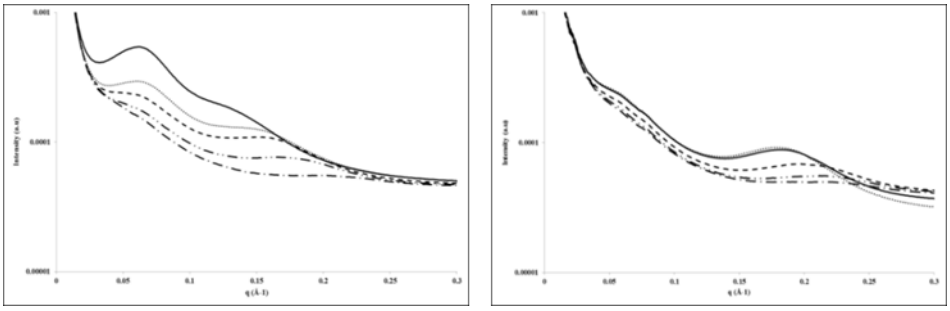

Figure 19. SAXS profile of untreated (left) and decalin treated (right) N212 membrane at 50 °C and 35 (-.-)), 50 (- ..-), 75 (- -), 85 (. . .) and 95% (--) RH at 60 % RH.

NMR study of membrane backbone. To understand the morphological changes evidenced by SAXS (previous annual report) and enhanced fuel cell performance, we characterized decalin treated membranes using solid state NMR. Motional modes near the experimental spin-lock frequency will increase relaxation rates i.e., smaller $T_{1\rho}$ values. The spectroscopic resolution provided by MAS allows for the distinction of fluorine signals from i) main-chain CF_2, ii) side-chain O-CF_2 and CF_3 and iii) side-chain S-CF_2 directly adjacent to the sulfonic acid group in the Nafion® membrane.

Overall $T_{1\rho}$ values in decalin treated membranes are shorter over the entire spectral frequency range compared to the untreated Nafion® for both main-chain and side-chain nuclei, which is attributed to more motional freedom and thus more routes for relaxation processes (Fig. 20). This reduction suggests that decalin treatment increases motional modes in both the backbone and side-chain moieties. This is direct evidence of interaction between the decalin and the hydrophobic portion of the polymer.

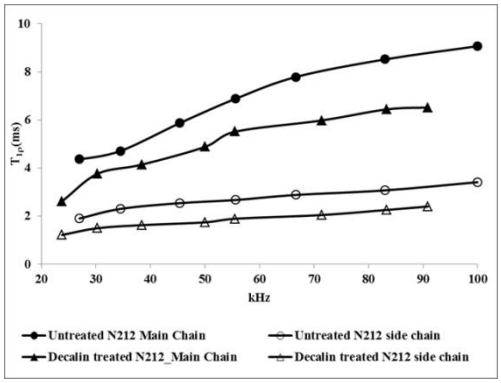

Figure 20. $T_{1\rho}$ for main-chain and side-chain fluorine for untreated and decalin treated N212 membranes as a function of frequency.

$T_{1\rho}$ values for fluorine atoms adjacent to the acid groups, which are solvated by water, are nearly identical for treated and untreated membranes. This implies that decalin does not interfere with the interplay between water and the ionic groups. These NMR experiments support SAXS results, which showed that decalin hampered the lamellar crystallite domain, implying a less ordered, more dynamic backbone. SAXS also showed that ionic clustering still occurred in decalin treated membranes, and NMR showed no effect on hydrophilic motions. PFG-NMR determination of the self-diffusion coefficients of several fuels including 1,4-pentanediol in Nafion™ membranes is ongoing.

Membrane vs. electrode treatment. Since the MEAs with decalin treated N212 membranes showed 85% increase in power density and substantially reduced hydrogen crossover in a H_2/air fuel cell at 60% RH, we tried to separate decalin effect on the PEM from its effect on the catalyst layers. Similar to the decalin treated N212, the fuel cell with decalin treated electrodes also exhibited increased (though to lesser extent) performance at low RH (Fig. 21). The voltage drop at higher currents can be attributed to diffusion losses in the electrode layer due to the presence of decalin. While the treated membranes showed a 40 mV higher open circuit voltage than the untreated ones, this effect was not observed with the decalin treated electrodes. This confirms that the increase in OCV for the decalin treated N212 is solely due to reduction in the hydrogen crossover and does not include mixed potential and oxide formation effects.

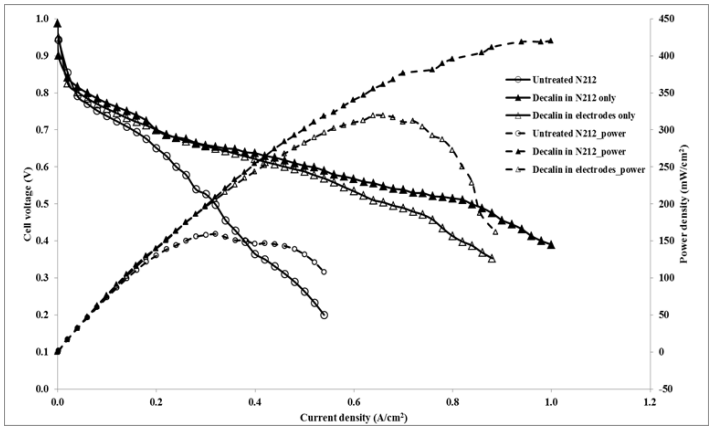

Figure 21. Fuel cell performance of untreated, decalin treated N212 membrane and decalin treated electrodes at 75 C and 60%

The observed improvement in performance with the decalin treated N212 and electrodes remained unchanged after operating the fuel cell under steady conditions for three days. Cyclic voltammetry confirms that a larger fraction of the platinum catalyst was electrochemically active for the decalin treated N212 and electrodes compared to the untreated N212 MEA. The improvement at low RH observed with both the treated membrane and the electrode painted with decalin suggests that even a hydrophobic skin formed during MEA fabrication enhances water retention in Nafion® resulting in high water sorption and proton conductivity consequently resulting in higher fuel cell power density at low RH.

IMPROVING MEMBRANE SELECTIVITY VIA MODIFICATION OF PROTON CONDUCTING MEDIA

We have demonstrated reduced fuel crossover and improved conductivity in multilayer membranes modified with hydroxymethyl imidazole.

In order to improve PEM selectivity, 4(5)-hydroxymethyl imidazole (ImOH) was added to Nafion 212. Through water sorption measurements, it was found that incorporation of ImOH into the membrane reduces water up-take meaning that a fully hydrated modified membrane contains less water than the unmodified membrane. Using small angle x-ray scattering (SAXS), it was also found that the modified membrane undergoes less swelling during hydration. These two measurements are consistent in that reducing water content in the membrane results in reduced swelling. As hydration of the membrane forms conductive channels through the membrane providing pathways for fuel transport through the membrane, by reducing water content and swelling we restrict the pathway for fuel transport. Conductivity results for Nafion® modified with hydroxymethylimidazole clearly demonstrate that the critical nature of the nitrogen base and its ratio to acidic groups (Fig. 22).

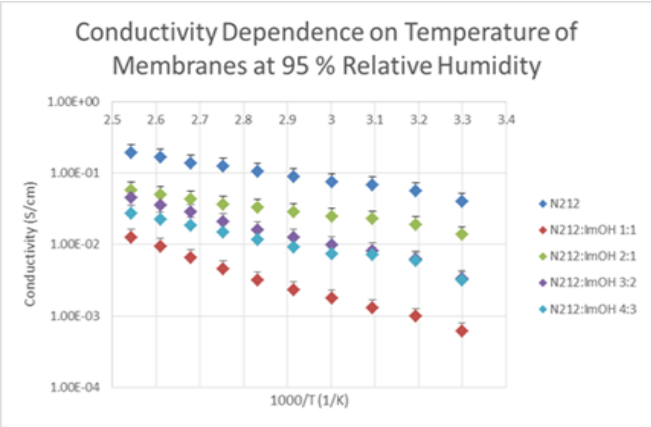

Figure 22. Conductivity vs. temperature for the control and four imidazole modified membranes at 95% relative humidity.

Using a direct methanol fuel cell as a control liquid fuel cell, the effects on fuel crossover are significant. In a DMFC at 60°C with a 1M methanol fuel, fuel crossover current with a modified membrane is 20 times less that for the unmodified membrane (Figure 23).

Unfortunately, the modified membranes result in a significant increase in charge transfer resistance (R_{CT}). By using a multilayered membrane (Figure 24), it is possible to isolate the modified layer from the electrodes and reduce the charge transfer resistance in the modified cell. From a qualitative look at the MEA impedance, it can be seen that the modified multilayer MEA has significantly 3-4 times less resistance to charge transfer than the modified single layer based on the size of the capacitive loop in the Nyquist plot.

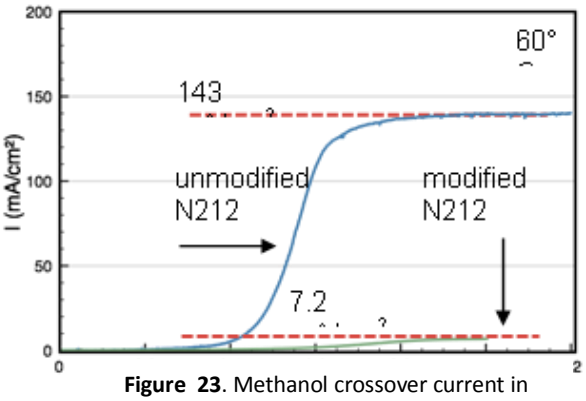

Figure 23. Methanol crossover current in DMFC shows significant reduction in crossover in modified Nafion membranes

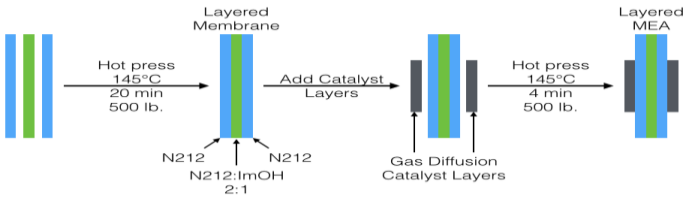

Figure 24. Assembly of multilayer membrane electrode assemblies

SUPPORTING AND TESTING ELECTROCATALYSTS ON CONDUCTING CARBON SURFACES

We investigated different ways to immobilize molecular electrocatalysts on a carbon surface and developed reliable methods providing high e=rate of electron transferand chemical stability.

Catalyst immobilization. We hypothesized that surface tethering of the catalyst would not impede interfacial electron transfer nor negatively impact the electrocatalytic activity. Various strategies' have been explored for attaching electrodehydrogenation catalysts to electrodes with the emphasis on chemically robust attachment and rapid transfer of electrons between the electrode and catalyst. We have chosen to target carbon electrodes because they are low cost, exhibit high stability at desired fuel oxidation potentials (~+0.2V vs. NHE), and have high surface area or porosity with a wide range of nanostructures (carbon black, nanotubes, graphene, etc.).

A highly controlled, tunable and scalable process to modify carbon surfaces has been developed.[93] Carbon samples are first pyrolyzed in forming gas (5% H_2 in N_2) to remove oxygen from the surface and then treated *in situ* at room temperature with a low vapor pressure of IN_3, forming surface azide groups (Fig. 25). Catalyst species with terminal ethynyl groups (-C≡CH) can then be covalently attached to the surface under ambient conditions in aqueous or organic solvents using standard "click" procedures catalyzed by a variety of Cu(I) complexes to yield up to a dense monolayer. The triazole linker between the surface and the catalyst promotes rapid electron transfer (>100s^{-1} at reversible potential) and less than 20% of the triazole linker is lost after 12 hours at 100°C in either 1M NaOH or 1M $HClO_4$. Alternatively, the azide groups can be reduced to amines and species attached by more conventional nucleophilic reactions.

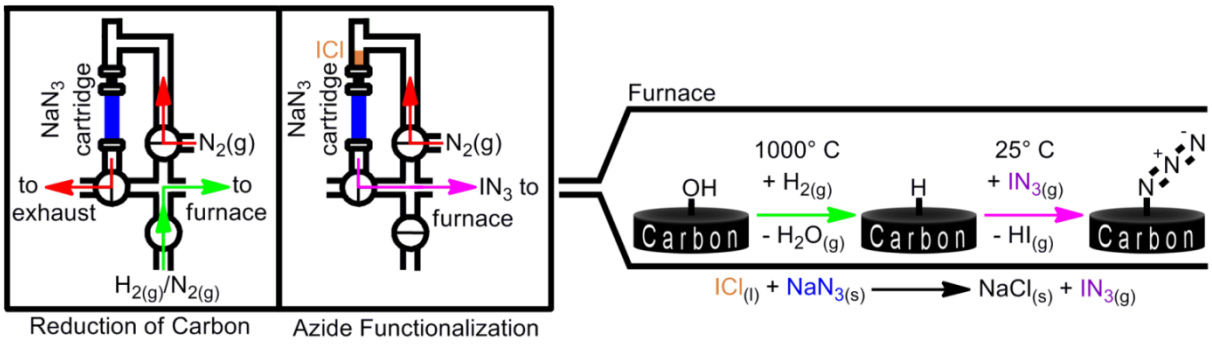

Figure 25. Azide functionalization occurs in a two-step procedure using IN_3 (*g*) gas generated by reaction of the vapor of ICl vapor with solid NaN_3.

The kinetics of the Cu (I)-catalyzed azide alkyne cycloaddition reactions at surfaces have been investigated on both azide-terminated carbon and on azide-terminated alkane thiol monolayers on gold. Cu(I) can be formed by the comproportionation of Cu(II) in the reactant solution and a metallic copper surface abutting the surface to be functionalized; the typical reaction time for surface functionalization is 1s with 1mM alkyne and 1 mM Cu(II). An optimized X-ray photoelectron spectroscopy method has been developed to follow the functional composition of the surface during the reaction sequence with elemental sensitivity of 0.1%.

We studied a model system in which azide-terminated thiol linkers of different lengths are chemisorbed on gold and the outer-sphere electrocatalyst, ferrocene (Fc) is attached by the "click" reaction. The oxidation of the model fuel, benzyl aniline, by surface immobilized Fc shows a 5-fold current enhancement with 4% coverage of ferrocene. We have extended these studies and covalently attached ethynyl-terminated ferrocene (Fc) to glassy carbon surfaces and further adapted the vapor-phase modification of carbon surfaces with azide groups to work on carbon powder (Vulcan XC-72R) so

that species with appended ethynyl groups (-C≡CH) can be covalently attached to practical carbon surfaces under ambient conditions. The reproducible, scalable, and chemically-specific azide functionalization of high surface area carbon Vulcan XC-72R powder with coverage of 1.4 x 10^{14} azides/cm^2, the highest functional group coverage on a porous carbon surface, was achieved by treatment with gaseous IN_3. Similar results were obtained using a spray coating technique that allowed catalysts (decamethyl ferrocene) as well as base modifiers (tetramethylguanidine) to be incorporated in the electrode layers and MEAs.

Catalyst support modification.

An easy and inexpensive hydrothermal reaction of carbohydrate polymerization followed by carbonization was developed to attach hydroxyl groups as a good chemical building block to the multi-walled carbon nanotube (MWCNT) surface. MEAs with MWCNT grafted with allyl group on the surface (Scheme 10) demonstrated a current density of 2.5 A/cm^2 compared to 1 A/cm^2 for conventional XR-72C support in a hydrogen fuel cell.

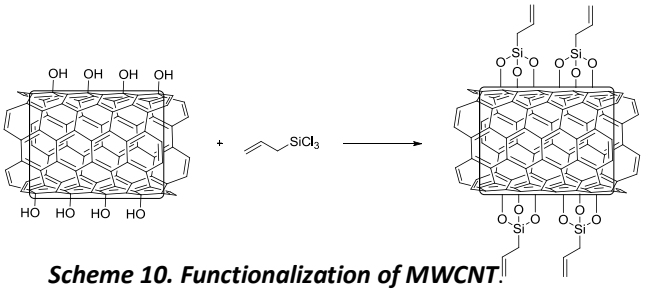

Scheme 10. Functionalization of MWCNT.

CONCLUSIONS

The vision of the Center for Electrocatalysis, Transport Phenomena and Materials for Innovative Energy Storage (EFRC-ETM) was the direct use of organic hydrides in fuel cells as virtual hydrogen carriers that generate stable organic molecules, protons, and electrons upon electro-oxidation and can be electrochemically charged by re-hydrogenating the oxidized carrier. Compared to a hydrogen-on-demand design that includes thermal decomposition of organic hydrides in a catalytic reactor, the proposed approach is much simpler and does not require additional dehydrogenation catalysts or heat exchangers. Further, this approach utilizes the advantages of a flow battery (i.e., separation of power and energy, ease of transport and storage of liquid fuels) with fuels that have system energy densities similar to current hydrogen PEM fuel cells. During EFRC program various types of electrocatalysts, classes of fuels, and membranes have been investigated. Two major EFRC challenges were electrocatalysis and transport phenomena. The electrocatalysis challenge as depicted by the horizontal flow of Fig. 26 addresses processes which occur at a single molecular catalyst (microscopic level) and involve electron and proton transfer between the organic liquid fuel (L and LH_n) and the catalyst. To form stable, non-radical dehydrogenation products from the organic liquid fuel, it is necessary to ensure fast transport of at least two electrons and two protons (per double bond formation). The same is true for the reverse hydrogenation reaction. The transport phenomena challenge addresses transport of electrons to/from the electrocatalyst and the current collector as well as protons across the polymer membrane. Additionally it addresses prevention of organic liquid fuel, water and oxygen transport through the PEM. In this challenge, the transport of protons or molecules involves multiple sites or a continuum (macroscopic level) and is represented as the vertical flow in Fig. 26. Water serves

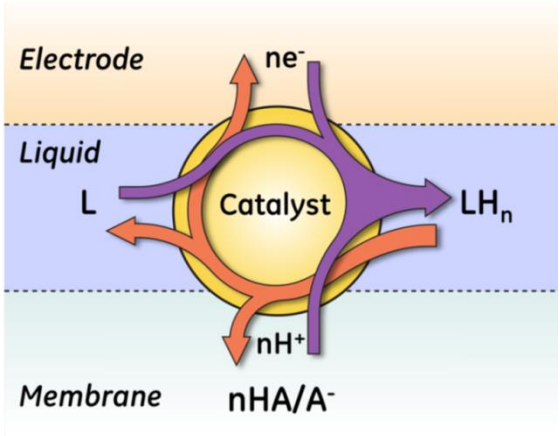

Figure 26. Electron and proton flows addressed by EFRC-ETM challenges of electrocatalysis and transport phenomena

as a proton conducting medium for the majority of known sulfonic acid based PEMs. It often interferes with redox processes or interacts with basic groups of many prospective organic liquid fuels. Therefore we studied proton transfer in water-limited or anhydrous PEMs in the presence of fuels.

One of the early goals of the EFRC-ETM was to develop criteria for fuel selection, which can be used in identifying candidate organic fuels. The approach was to close the knowledge gap through understanding thermodynamic and electrochemical properties, and to investigate the compatibility of different fuel and membrane classes. For different fuel classes (e.g., carbocyclic fuels, O- and N-heterocyclic fuels and oxygenates) we developed and verified an accurate computational tool for the calculation of thermodynamic properties and fuel redox potentials. This tool enabled the identification of potential fuels with high energy densities (1100 - 1650 Wh/L), some of which have theoretical open circuit potentials higher than that of the hydrogen fuel cell. We also found that the theoretical maximum efficiency of fuel cells using organic fuels is in the range of 93 – 95% at 80°C (83% for hydrogen fuel cells) the organic fuels advantage increases with temperature. In principle, organic fuel cells may be competitive for mobile energy storage (e.g. for a 300 mile range car powered by the decalin/naphthalene couple, the fuel tank size would be ~16.5 gal) as well as stationary applications owing to their high OCP and theoretical efficiencies.

The study of liquid organic fuel electrooxidation allowed for determination of the structure property relationship of the organic liquid fuel and the oxidation potential, as well as the nature of the products formed by electrooxidation in the absence of a catalyst at a bare electrode. It was shown that the addition of substituents can alter the oxidation potential of organic liquid fuels and is more pronounced when in conjugation with the oxidation site. A mechanism of negative potential shift and current increase in the presence of a base was elucidated and quantified. Therefore, bases can be employed to enhance the rate of the electrooxidation and lower the oxidation onset potential for liquid organic fuels.

To select proton conducting membranes compatible with selected fuels, we investigated factors controlling transport and selectivity in membranes. Using candidate organic fuels, we closed a large knowledge gap with respect to understanding organic liquid fuel/membrane interactions and the mechanism of proton and fuel transport in water-limited or anhydrous PEMs. We have studied transport mechanisms to establish design criteria for membrane materials capable of selective transport of protons in competition with molecules of organic liquid fuels or water. The approach was to characterize the dynamic relaxation, mechanical and morphological properties of commercially available acidic membranes plasticized with candidate fuels in order to understand the effect of fuel-electrolyte-polymer interactions. We found that hydrocarbon cyclic fuels interact with the hydrophobic polymer backbone changing the membrane morphology in such a way that preserves high proton conductivity at low relative humidities and reduces the hydrogen crossover. This effect results in substantial power density increase for hydrogen-oxygen fuel cells.

The EFRC-ETM relied on theoretical support to gain insight into reaction mechanisms, and therefore have developed theoretical models for redox potentials, both of fuel molecules and electrocatalysts. In the area of electrocatalysis, developed computational tools were used for calculation of redox potentials of transition metal complexes and demonstrated the ability to predictably adjust those redox potentials using structure activity relationships within at least 600 mV range. These tools were also used to evaluate pathways for different catalytic cycles and illustrated the benefit of using non-innocent ligands for two proton/two electron transfer in the electrocatalytic dehydrogenation of chemical fuels.

The use of outer sphere electrocatalysts (ferrocenes, NNN cobalt complexes) resulted in formation of mostly radical products of one-electron oxidation. Addition of a strong base only slightly improved reaction selectivity towards dehydrogenation.

We found that quinones with high oxidation potential can be used as electrocatalysts in oxidation of N-containing fuels via formation of pi-complexes with substrates. While this strategy successfully demonstrates the effectiveness of using an inner sphere electrocatalyst (selective product formation) the relatively high redox potential and slow reaction kinetics of quinones suggests that they are not practical electrocatalysts in the context of an organic fuel cell.

Our initial hypothesis of using thermal dehydrogenation catalysts as electrocatalysts turned out to be only partially true. In many cases these catalysts were inactive in electrooxidation. Computational study of electrooxidation mechanisms indicated that the formation of intermediate species with negative redox potentials broke the catalytic cycle.

A mechanism of electrocatalysis by rhodium(II) cationic complexes in the dehydrogenation of formate (a model system) established via identification of all intermediates revealed a two electron redox process. Theoretical and electrochemical analyses of several substituted bipyridyl derivatives of the rhodium(III) hydride established an inverse dependence of the acidity and hydricity on the nature of the chelating ligand. This theoretical model predicted a ligand environment which, when implemented, enhanced the overall electrocatalytic efficiency of the rhodium(III) catalyst system.

EFRC-ETM developed iridium catalysts with non-innocent ligands that showed excellent selectivity and Faradaic yields in the oxidation of alcohols. The iridium system demonstrated the desired separation of protons and electrons with a homogeneous catalyst system used in the electrochemical dehydrogenation of fuels.

Understanding parameters controlling activity in both directions (reversibility) is extremely important for development rechargeable fuel cells. With the current iridium system, the concept of utilizing microscopic reversibility was extended to electrocatalysis by employing the same electrocatalyst precursor with a base/conjugate acid pair in the presence of the appropriate metallocenes as oxidizing and reducing agents for the electrochemical dehydrogenation/hydrogenation of a fuel/spent fuel combination has been demonstrated.

Despite these recent promising findings with an iridium electrocatalyst, the high cost and limited availability of PGMs still present a major hindrance in wide spread acceptance of fuel cell technology. Therefore, we investigated catalysts based upon more abundant and less expensive, non-precious metal catalysts including nickel, cobalt, and copper in electrochemical dehydrogenation and hydrogenation reactions. We have separately shown electro-dehydrogenation and -hydrogenation reactions with first row transition metal electrocatalysts, nickel pincer complexes. The microscopic reversibility principle was also demonstrated in reversible acceptorless dehydrogenation of alcohols effectively catalyzed by an iron complex with non-innocent ligand.

To make molecular complexes of transition metals practical for the use in organic fuel cells, we studied their immobilization of model and practical conductive carbon surfaces. The method of attaching reactive azide groups to various carbon surfaces for tethering catalysts through “click” chemistry have been greatly improved. As a result, very high surface concentrations of tethered metal complexes were achieved. This technique has been used to modify flow cell electrodes in order to incorporate catalysts as well as mediators and bases. Furthermore, it has been demonstrated that the redox potentials and rates of electron transfer of electrocatalysts tethered in this fashion to glassy carbon electrodes are not impacted.

The further work based on the EFRC-ETM results can be eventually translated into design criteria for the envisioned innovative energy storage and delivery system.

6. Products Developed or Technology Transfer Activities

A. Publications and Conference Proceedings

i) Publications

1. Crabtree, Robert H Electrochemical and Photoelectrochemical Conversion of CO2 to Fuels, Encyclopedia of Inorganic Chemistry, (2011). [10.1002/0470862106]
2. Crabtree, Robert H Multifunctional Ligands in Transition Metal Catalysis , New Journal of Chemistry, 35, 18–23 (2011). [10.1039/C0NJ00776E]
3. Soloveichik, Grigorii Batteries for Large Scale Energy Storage, Annual Review of Chemical and Biomolecular Engineering, 2, (2011). [10.1146/annurev-chembioeng-061010-114116]
4. Luca, Oana R; Wang, Ting; Konezny, Steven J; Crabtree, Robert H; and Batista, Victor S. DDQ as an Electrocatalyst for Amine Dehydrogenation, New Journal of Chemistry, 35, 998-999 (2011). [10.1039/C0NJ01011A]
5. Rozenel, Sergio S; Kerr, John B; and Arnold, John Metal complexes of Co, Ni and Cu with the pincer ligand HN(CH(2)CH(2)P(i)Pr(2))(2): preparation, characterization and electrochemistry, Dalton Transactions, 40, 10397-10405 (2011). [10.1039/C1DT10599J]
6. Konezny, Steven J; Doherty, Mark D.; Luca, Oana R; Crabtree, Robert H; Soloveichik, Grigorii; and Batista, Victor S. Reduction of Systematic Uncertainty in DFT Redox Potentials of Transition-Metal Complexes, J. Phys. Chem C, 116, 6349–6356 (2012). [10.1021/jp300485t]
7. Crabtree, Robert H Resolving Heterogeneity Problems and Impurity Artifacts in Operationally Homogeneous Transition Metal Catalysts, Chem. Rev., 112, 1536–1554 (2012). [10.1021/cr2002905]
8. Araujo, C. Moyses; Doherty, Mark D.; Konezny, Steven J; Luca, Oana R; Usyatinsky, Alex; Grade, Hans; Lobkovsky, Emil B.; Soloveichik, Grigorii; Crabtree, Robert H; and Batista, Victor S. Tuning redox potentials of bis(imino)pyridine cobalt complexes: an experimental and theoretical study involving solvent and ligand , Dalton Transactions, 41, 3562 - 3573 (2012). [10.1039/C2DT12195F]
9. Luca, Oana R; Konezny, Steven J; Blakemore, James D; Colosi, Dominic M.; Saha, Shubhro; Brudvig, Gary W.; Batista, Victor S.; and Crabtree, Robert H A tridentate nickel pincer for aqueous electrocatalytic hydrogen production, New J. Chem., 36, 1149 – 1152 (2012). [10.1039/C2NJ20912H]
10. Batista, Victor S.; Crabtree, Robert H; Konezny, Steven J; Luca, Oana R; and Praetorius, Jeremy M. Oxidative Functionalization of Benzylic C-H Bonds by DDQ , New J. Chem., 36, 1141 - 1144 (2012). [10.1039/c2nj40021a]
11. Luca, Oana R.; Blakemore, James D; Konezny, Steven J; Praetorius, Jeremy M.; Schmeier, Timothy J.; Hunsinger, Glendon B.; Batista, Victor S.; Brudvig, Gary W.; Hazari, Nilay; and Crabtree, Robert H Organometallic Ni Pincer Complexes for the Electrocatalytic Production of Hydrogen, Inorg. Chem., 51, 8704–8709 (2012). [10.1021/ic300009a]
12. Araujo, C. Moyses; Simone, D.; Konezny, Steven J; Shim, Aaron; Crabtree, Robert H; Soloveichik, Grigorii; and Batista, Victor S. Fuel selection for a regenerative organic fuel cell/flow battery: thermodynamic considerations, Energy & Environmental Science, 5, 9534 – 9542 (2012). [10.1039/C2EE22749E]

13. Stenehjem, Eric D.; Ziatdinov, Vadim R.; Stack, T. Daniel P.; and Chidsey, Christopher E. D. Gas-Phase Azide Functionalization of Carbon, J. Amer. Chem. Soc., 135, 1110-1116 (2013). [10.1021/ja310410d]
14. Peters, Andrea; Rainka, Matthew P.; Krishnan, Lakshmi; Laramie, Sydney; Dodd, Matthew; and Reimer, Jeffrey A. Electrochemical Characterization of Hydrogen-Bonding Complexation Between Indoline and Nitrogen Containing Bases , J. Electroanal. Chem., (2013). [10.1016/j.jelechem.2012.12.006]
15. Luca, Oana R; and Crabtree, Robert H Redox-Active Ligands in Catalysis, Chem. Soc. Rev., 42, 1446-1459 (2013). [10.1039/C2CS35228A]
16. Eisenstein, Odile; and Crabtree, Robert H Outer sphere hydrogenation catalysis , New J. Chem., 37, 21-27 (2013). [10.1039/C2NJ40659D]
17. Luca, Oana R; Thompson, Bennett A; Takase, Michael K; and Crabtree, Robert H Synthesis and Electrochemistry of a Series of Cyclopentadienyl Ni N-Heterocyclic Carbene Compounds, J. Organomet. Chem., 730, 79-83 (2013). [10.1016/j.jorganchem.2012.10.038]
18. Crabtree, Robert H Abnormal, Mesoionic and Remote N-H heterocyclic Carbene Complexes, Coord. Chem. Rev., 257, 755-766 (2013). [10.1016/j.ccr.2012.09.006]
19. Rainka, Matthew P.; Peters, Andrea; and Soloveichik, Grigorii Base Effects on Electrochemical Oxidation of Indoline, Int. J. Hydrogen Energy, 38, 3773-3777 (2013). [10.1016/j.ijhydene.2011.12.009]
20. Luca, Oana R; Huang, Dana; Takase, Michael K; and Crabtree, Robert H A redox-active cyclopentadienyl Ni complexes with quinoid N-heterocyclic carbene ligands for the electrocatalytic hydrogen release from chemical fuels, New Journal of Chemistry, 37, 3402-3405 (2013). [10.1039/c3nj00276d]
21. Luca, Oana R; Konezny, Steven J; Paulson, Eric K.; Habib, Fatemah; Luthy, Kurt M.; Murugesu, Muralee; Crabtree, Robert H; and Batista, Victor S. Study of an S = 1 Ni(II) pincer electrocatalyst precursor for aqueous hydrogen production based on paramagnetic 1H NMR, Dalton Transactions, 42, 8802-8807 (2013). [10.1039/c3dt50528f]
22. Habib, Fatemah; Luca, Oana R; Vieru, Veacheslav; Shiddiq, Muhandis ; Korobkov, Ilia; Gorelsky, Serge I. ; Takase, Michael K; Chibotaru, Liviu F. ; Hill, Stephen; Crabtree, Robert H; and Murugesu, Muralee Influence of the Ligand Field on Slow Magnetization Relaxation versus Spin Crossover in Mononuclear Cobalt Complexes, Angew. Chem. Int. Ed., 52, 11290–11293 (2013). [10.1002/anie.201303005]
23. Driscoll, Peter F.; Deunf, Elise; Rubin, Leah; Arnold, John; and Kerr, John B lectrochemical Redox Catalysis for Electrochemical Dehydrogenation of Liquid Hydrogen Carrier Fuels for Energy Storage and Conversion, J. Electrochem. Soc, 160, G3152-G3158 (2013). [10.1149/2.024307jes]
24. Bonitatibus, Jr., Peter J.; Rainka, Matthew P.; Peters, Andrea; Simone, D.; and Doherty, Mark D. Highly selective electrocatalytic dehydrogenation at low applied potential catalyzed by an Ir organometallic complex, Chem. Commun., 49, 10581 - 10583 (2013). [10.1039/C3CC46051G]
25. Soloveichik, Grigorii Regenerative Fuel Cells for Energy Storage , Proceedings of the IEEE, 102, 964-975 (2014). [10.1109/JPROC.2014.2314955]
26. Doherty, Mark D.; Konezny, Steven J; Batista, Victor S.; and Soloveichik, Grigorii Electrochemical Reactions of Pincer Rhodium(I) Complexes, J. Organomet. Chem., 762, 94-97 (2014). [10.1016/j.jorganchem.2013.10.045]
27. Chakraborty, Sumit; Brennessel, William; and Jones, William D A Molecular Iron Catalyst for the Acceptorless Dehydrogenation and Hydrogenation of of N-Heterocycles, J. Am. Chem. Soc., 136, 8564–8567 (2014). [10.1021/ja504523b]

28. Soloveichik, Grigorii Liquid fuel cells, Beilstein J. Nanotechnology, 5, 1399-1418 (2014). [10.3762/bjnano.5.153]
29. Ding, Wendu; Negre, Christian F. A.; Vogt, Leslie; and Batista, Victor S. Single Molecule Rectification Induced by the Asymmetry of a Single Frontier Orbital, J. Chem. Theory Comput., 10, 3393–3400 (2014). [10.1021/ct5004687]
30. Siclovan, Oltea; Zappi, Guillermo; and Soloveichik, Grigorii High-Temperature Cyclic Voltammetry in Non-Aqueous Solvents, ECS Electrochemistry Letters, 3, H1-H3 (2014). [10.1149/2.0051412eel]
31. Chakraborty, Sumit; Lagaditis, Paraskevi O.; Forster, M.; Bielinski, Elizabeth A.; Hazari, Nilay; Holthausen, Max C.; Jones, William D; and Schneider, Sven Well-Defined Iron Catalysts for the Acceptorless Reversible Dehydrogenation-Hydrogenation of Alcohols and Ketones, ACS Catalysis, 4, 3994-4003 (2014). [10.1021/cs5009656]
32. Luca, Oana R; Konezny, Steven J; Hunsinger, Glendon B.; Muller, Peter; Takase, Michael K; and Crabtree, Robert H Ni Complexes of Redox-Active Pincers with Pendant H-bonding Sites as Precursors for Hydrogen Production Electrocatalysis, Polyhedron, 82, 2-6 (2014). [10.1016/j.poly.2013.12.003]

ii) Conference proceedings

1. P. F. Driscoll, E. Deunf, L. Rubin, O. Luca, R.H. Crabtree, C.E.D. Chidsey, J. Arnold, J. Kerr, Redox Catalysis for Dehydrogenation of Liquid Hydrogen Carrier Fuels for Energy Storage and Conversion Electrocatalysts for Fuel Cells, ECS Trans. 2011 35(28): 3-17; doi:10.1149/1.3641814
2. P. F. Driscoll, E. Deunf, L. Rubin, J. Arnold, J. Kerr, Electrochemical Redox Catalysis for Electrochemical Dehydrogenation of Liquid Hydrogen Carrier Fuels for Energy Storage and Conversion, ECS, Trans. 2013, submitted.
3. G.W. Yeager, L. Krishnan, T. A. Early, T.C. Zhang, and M. R. LaTorre, Novel Polybenzimidazole-Phosphoric Acid Membranes for Fuel Cell Applications, ECS Trans. 2013 50(2): 1179-1191; doi:10.1149/05002.1179ecst
4. K. T. Clark, L. Krishnan G.W. Yeager, and J. Kerr, Membrane Science for Liquid Organic Fuel Cells, ECS Trans. 2013 50(2): 2129-2137; doi:10.1149/05002.2129ecst
5. D. Kellenberger, E. Deunf, J. Arnold, J. Kerr, Electrocatalytic Oxidation of Formate with Rh(III) Electrocatalysts and Related Reactivity for PEM Fuel Cell Applications, Preps. Pap.-Am. Chem. Soc., Div. Energy Fuels 2013, 58 (1), in press.

B. Website

Our EFRC hosts a website, www.ge.com/efrc and GE members of the EFRC can also blog to http://ge.geglobalresearch.com/blog/ and inform the public about scientific discoveries related to the EFRC-ETM.

C. Networks or Collaborations Formed

We have developed a strong network with our External Advisory Board members: Dr. Craig Gittleman (GM), Prof. Bob Savinell (CWRU), Dr. Tom Zawodzinski (ORNL/UTenn), Dr. R. Morris Bullock (PNNL) and Prof. P. Pintauro (Vanderbilt University).

We have formed collaborations with following research groups.

University Montpellier, France (O. Eisenstein) – computational chemistry
University of Barcelona, Spain (D. Balcells) - computational chemistry
University of Maryland (A. Vedernikov) – Pt hydride intermediates
Stanford University (R. Waymouth, T. Jaramillo, D. Stack) – electrocatalysis
University of Rochester (W. Jones) – Ni pincer complex electrocatalysts
Hebrew University (D. Gelman) – Ir pincer complexes in electrocatalysis
University of New Mexico (P. Atanassov) – dehydrogenation electrocatalysts
SUNY Albany (C. Scholes) – EPR study of Ir intermediates
Brookhaven National Lab (E. Fujita) – pulse radiolysis study of Ni intermediates
University of Tennessee Knoxville (A. Papandrew) – novel PEM membranes
Clark University (Prof. S. Granados-Focil) – novel PEM membranes
University of Toronto (R. Morris) – Fe transfer dehydrogenation catalysts
University of Oregon (S.-Y. Liu) – borazine based organic fuels
University of Ottawa (M. Murugesu) – magnetism measurements
US Berkeley (R. Segalman, J. Reimer) – polymer membrane chemistry
Danish Power Systems (T. Stenberg) – PBI based PEMs
Oorja Protonics, INC. (Fremont, CA) - application of EFRC membrane for DMFC
Yale University (G. Brudvig, N. Hazari) - electrocatalysis by first row transition metal complexes.

We established cooperation (via LBNL) with Oorja Protonics, Freemont, CA based company with focus on MEA development for improved Direct Methanol Fuel Cell (DMFC) and Liquid-fed Fuel Cell systems. It is anticipated that EFRC technological innovations in electrocatalysts and PEMs would lead to faster commercialization of the Liquid Fuel Cells in several applications such as range-extenders for various electric vehicle platforms.

D. Inventions/Patent Disclosures

1. R.H. Crabtree, O. Luca, “Organocatalysis for Virtual Hydrogen Storage”, Yale University Docket OCR5410 of 7/2/2010)
2. G.L. Soloveichik, L.N. Lewis, R.H. Crabtree, “Use of pi-conjugated heterocyclic materials for electrochemical energy storage”, GE GRC Patent docket #245349, April 2010.
3. O.R. Luca and R.H. Crabtree, “Nickel pincers for proton and heterocycle reduction”, Yale University, Docket OCR5613 of 2/17/2011.
4. O.Siclovan. T.Early, G. Soloveichik “Electrocatalyst for oxidation of heterocyclic compounds”, GE GRC, Docket RD250974 of 2/21/2011.
5. G. Yeager, “Polyazoles and composite membranes comprising them”, GE GRC, Docket RD 254556, November 2011.
6. G. Yeager, G. Soloveichik, L. Krishnan, “Modified perfluorosulfonic acid proton exchange membranes” GE GRC, Docket RD 254556, March 2012.
7. O.R. Luca and R.H. Crabtree “VIRTUAL HYDROGEN STORAGE PROCESSES AND RELATED CATALYSTS AND SYSTEMS”, Yale University, WIPO Patent Application PCT/US12/25415

E. Other Products

i) Invited and Keynote Lectures

Author(s)	Title	Institution/ Conference	Location	Month/Year
G.L. Soloveichik	GE Energy Storage Vision For Mobile & Stationary Applications	2009 Advanced Energy Conference "Solutions to a Global Crisis"	Hauppauge, NY	11/2009
G.L. Soloveichik	New energy storage system combining a flow battery and a fuel cell	GE Global Electrochemistry Symposium	Niskayuna, NY	3/2010
R.H. Crabtree	Climate Change and our Energy Future (3eme cycle lecture series)	University of Fribourg	Fribourg, Switzerland	12/2009
R.H. Crabtree	The climatic history of the Earth	University of Basel	Basel, Switzerland	12/2009
R.H. Crabtree	Climate Change and our Energy Future (Kosolapoff Award lecture)	Auburn University	Auburn, AL	4/2010
R.H. Crabtree	Climate Change and our Energy Future (Stauffer lecture)	University of Southern California	Los Angeles, CA	4/2010
V.S. Batista	Natural and artificial photosynthesis	Universita Della Calabria	Arcavacada di Rende, Italy	1/2010
V.S. Batista	Studies of oxomanganese complexes for natural and artificial photosynthesis	University of Michigan	Ann Arbor, MI	1/2010
R.H. Crabtree	Virtual Hydrogen Storage	Yale West Campus Energy Symposium	New Haven, CT	2/1010
V.S. Batista	The MP/SOFT methodology for simulations of multi-dimensional quantum dynamics	University of Maryland	College Park, MD	3/2010
V.S. Batista	Coherent control with sequences of unitary phase kick pulses	239th ACS National Meeting,	San Francisco, CA	3/2010
V.S. Batista	Studies of oxomanganese complexes for natural and artificial photosynthesis	MIT	Cambridge, MA	3/2010
R.H. Crabtree	Climate Change and our Energy Future	University of New Hampshire	Durham, NH	3/2010
V.S. Batista	Studies of oxomanganese complexes for natural and artificial photosynthesis	Pennsylvania State University	University Park, PA.	4/2010

C.E.D. Chidsey	'Click' Attachment of Electrocatalysts to Carbon	ECHEMS meeting	Sandbjerg, Denmark	6/2010
G.L. Soloveichik	Energy Storage: From Fuel Cells to Flow Batteries?	ASME 2010 8th International Fuel Cell Science, Engineering & Technology Conference	Brooklyn, NY	6/2010
R.H. Crabtree	Hydrogen Storage (Job Memorial Lecture)	Memorial University	St. John's, Newfoundland	7/2010
R.H. Crabtree	More Tools for the GC Toolbox: Selective Oxidations, Green Chemistry	Green Chemistry Gordon Conference	Davidson College, NC	7/2010
G.L. Soloveichik	Hydride fuel cells: from solid to liquid fuel	MH2010 International Symposium on Metal-Hydrogen Systems	Moscow, Russia	7/2010
V.S. Batista	Solar energy conversion and storage	240th ACS National Meeting	Boston, MA	8/2010
V.S. Batista	Solar energy conversion and storage	XV International Workshop on Quantum Systems in Chemistry and Physics	Cambridge, UK	9/2010
V. R. Ziatdinov, C. E. D. Chidsey	Vapor deposition of azide on carbon surfaces	218th ECS Meeting	Las Vegas, NV	10/2010
G. Soloveichik, G. Zappi	Electrocatalysis, Transport Phenomena, and Materials for Innovative Energy Storage	218th ECS Meeting	Las Vegas, NV	10/2010
V.S. Batista	Solar energy conversion and storage	41st Winter Colloquium on the Physics of Quantum Electronics	Snowbird, UT	1/2011
V.S. Batista	Studies of oxomanganese complexes for natural and artificial photosynthesis	2011 Gordon Research Conference on Renewable Energy: Solar Fuels	Ventura, CA	1/2011
O.R. Luca	Applications of Nickel pincers and high potential quinones for Virtual Hydrogen Storage	Yale Climate and Energy Institute Congress	New Haven, CT	2/2011

R.H. Crabtree	Selective catalytic oxidations of water and of CH bonds by iridium and manganese	241st ACS Meeting	Anaheim, CA	3/2011
R.H. Crabtree	Selective catalytic oxidations of water and of CH bonds by iridium and manganese	Netherlands Catalysis and Chemistry Conference	Noordwijkerhout, Netherlands	3/2011
V.S. Batista	Studies of PCET in Natural and Artificial Photosynthesis	2011 Fall ACS Meeting	Denver, CO	8/2011
V.S. Batista	Modeling Electrocatalytic Processes for Virtual Hydrogen Fuel Production	Role of computations in energy discovery symposium	Niskayuna, NY	8/2011
V.S. Batista	Studies of PCET in Natural and Artificial Photosynthesis	International Conference PCET 2011	Loire Valley, France	10/2011
G. Soloveichik	From metal hydride complexes to virtual hydrogen storage	Caulton Inorganic Chemistry Symposium	Bloomington, IN	10/2011
V.S. Batista	Studies of PCET in Natural and Artificial Photosynthesis	At the Interface of Natural and Artificial Photosynthesis	Albany, NY	11/2011
R.H. Crabtree	Hydrogen storage in organic liquids	2012 ACS Spring Meeting	San Diego, CA	3/2012
R.H. Crabtree	Organometallic Iridium Catalysts for Synthesis and Energy Research: Heteroarene hydrogenation, Stereoretentive Hydroxylation of C-H Bonds and Water Oxidation	Scripps Institute (Distinguished Lecturer Series)	San Diego, CA	4/2012
R.H. Crabtree	Organometallic Iridium Catalysts for Synthesis and Energy Research	Conference of 'Grupo Especializado en Química Organometálica' of Royal Chem. Soc. of Spain (Opening plenary lecture)	Castellón, Spain	6/2012
R.H. Crabtree	Organometallic Iridium Catalysts for Synthesis and Energy Research	Universitat Rovira i Virgili	Tarragona, Spain	6/2012
G. Soloveichik	Rechargeable Direct Organic Fuel Cells: Challenges	Fuel Cells Gordon Research Conference	Smithfield, RI	8/2012

V. Batista	Inverse Design of Electrocatalysts for Virtual Hydrogen Fuel Cells	Fuel Cells Gordon Research Conference	Smithfield, RI	8/2012
P.J. Bonitatibus Jr.*, G. Soloveichik, I. Warnke, A. Peters, D. Simone	Strategies for Homogeneous Electrocatalytic Dehydrogenation	244th ACS National Meeting & Exposition	Philadelphia, PA	8/2012
V. Batista	The Materials Inverse Design Problem	244th ACS National Meeting & Exposition	Philadelphia, PA	8/2012
R.H. Crabtree	Organometallic Precatalysts for Oxidation of Water and Alkyl CH Bonds	25th Intl. Conference on Organometallic Chemistry	Lisbon, Portugal	9/2012
V. Batista	The Materials Inverse Design Problem	Boston College	Boston, MA	9/2012
R.H. Crabtree	Catalysts for CH and Water Oxidation	University of Connecticut	Storrs, CT	10/2012
R.H. Crabtree	Water splitting, CH functionalization & energy storage with homogeneous catalysts	University of Wisconsin (McElvain lecture)	Madison, WI	1/2013
G. Soloveichik	Selection of Fuels for Direct Rechargeable Liquid Fuel Cell	2013 Spring MRS Meeting	San Francisco, CA	4/2013
J. Arnold*, D. Kellenberger, E. Deunf, J. Kerr	Electrocatalytic oxidation of formate with Rh(III) electrocatalysts and related reactivity for PEM fuel cell applications	245th ACS National Meeting & Exposition	New Orleans, LA	4/2013
V. Batista	Inverse Design of Electrocatalysts for Virtual Hydrogen Fuel Cells	MIT	Cambridge, MA	4/2013
R.H. Crabtree	Some Ni Pincers and Ir 'unpincers'	CSC Meeting	Quebec City, Canada	5/2013
R.H. Crabtree	Organometallic Iridium Catalysts for Synthesis and Energy Research: Heteroarene hydrogenation, Stereoretentive Hydroxylation of C-H Bonds and Water Oxidation	University of Utah	Logan, UT	9/2013

R.H. Crabtree	Homogeneous Catalysts for Green Applications	Yale University	New Haven, CT	11/2013
J. Kerr	Liquid Organic Hydrogen Carrier Technology for Energy Storage and Conversion	Gordon Research Conference on Batteries	Ventura, CA	3/2013
C.M. Araujo	Fuel-design for a novel regenerative organic fuel cell/flow battery	Challenges in Chemical Renewable Energy	Cambridge, UK	9/2013
J. Kerr	Polymer Electrolytes for Fuel Cell Separators and Electrodes	Penn State University	State College, PA	11/2013
R.H. Crabtree	Anchors and Catalysts for Solar Energy Applications	University of York	York, UK	3/2014
R.H. Crabtree	Anchors and Catalysts for Energy Applications	University of Nottingham	Nottingham, UK	3/2014
R.H. Crabtree	Anchors and Catalysts for Energy Applications	University of Bristol	Bristol, UK	3/2014
R.H. Crabtree	Anchors and Catalysts for Energy Applications	University of Oxford	Oxford, UK	4/2014
R.H. Crabtree	Anchors and Catalysts for Energy Applications	Imperial College London	London, UK	4/2014
R.H. Crabtree	Anchors and Catalysts for Energy Applications	Royal Chemical Society	Burlington House, UK	4/2014
G. Soloveichik	Electrocatalysis Challenge in Direct Rechargeable Liquid Fuel Cell	MRS Fall Meeting	Boston, MA	12/2013

ii) Other publications

Books

1. Crabtree, RH, The Organometallic Chemistry of the Transition Metals 5th ed., 2009
2. Crabtree, RH, “Electrochemical and Photoelectrochemical Conversion of CO_2 to Fuels”, in Energy Production and Storage – Inorganic Chemical Aspects, Crabtree RH (ed), Wiley, Chichester, 2010.
3. Book chapter "Polymer Materials for Charge Transfer in Energy Devices" by Kerr, John; Miller, Adam; Zhu, Xiaobing; Potrekar, Ravindra in ACS Books “Polymers for Energy Storage and Delivery: Polyelectrolytes for Batteries and Fuel Cells”, Manuscript ID: bk-2011-00471y

iii) Awards

P. Palomaki, a summer intern at GE from RPI, won the GE Early Identification Award 2010
R.H. Crabtree received the 2010 Kosolafoff Award (ACS and Auburn University)
S. Saha, a high school student in the Batista Lab was honored as an 2010 Intel STS finalist
R.H. Crabtree inducted into the American Academy of Arts & Sciences – 2011
O. Luca selected to be Author of the Month by the New Journal of Chemistry - May 2012
R.H. Crabtree elected ACS Fellow
R.H. Crabtree awarded King Lectureship (University of Georgia) - 2011
R.H. Crabtree elected IUPAC Fellow - 2013
R.H. Crabtree received the Royal Society of Chemistry 2013 Centenary Award
R.H. Crabtree awarded McElvain Lectureship (University of Wisconsin, Madison) - 2013
R.H. Crabtree - Yale Postdoctoral Mentoring Award - 2014
R.H. Crabtree - Siedle Lecture (Indiana University) - 2014

Technologies/Techniques

We have developed high temperature (up to 150^{o}C) electrochemistry method. We have developed a new flow cell and new bulk electrolysis cell that allows obtaining data with excellent reproducibility.

EFRC Alumni

The staffing spreadsheet is provided in a separate Excel spreadsheet.

Acknowledgment: "This material is based upon work supported by the Department of Energy, Office of Science under award Number DE-SC0001055."